SIAM J. SCI. COMPUT.
Vol. 20, No. 5, pp. 1753–1777

NUMERICAL APPROXIMATION OF OPTIMAL FLOW CONTROL PROBLEMS BY A PENALTY METHOD: ERROR ESTIMATES AND NUMERICAL RESULTS*

L. S. HOU† AND S. S. RAVINDRAN‡

Abstract. The purpose of this paper is to present numerically convenient approaches to solve optimal Dirichlet control problems governed by the steady Navier–Stokes equations. We will examine a penalized Neumann control approach for solving Dirichlet control problems from numerical and computational points of view. The control is affected by the suction or injection of fluid through the boundary or by boundary surface movements in the tangential direction. The control objective is to minimize the vorticity in the flow or to drive the velocity field to a desired one. We develop sequential quadratic programming methods to solve these optimal control problems. The effectiveness of the optimal control techniques in flow controls and the feasibility of the proposed penalized Neumann control approaches for flow control problems are demonstrated by numerical experiments for a viscous, incompressible fluid flow in a two-dimensional channel and in a cavity geometry.

Key words. flow control, sequential quadratic programming method, Navier–Stokes equations, finite elements, vorticity, optimization

AMS subject classifications. 93B40, 49M05, 76D05, 49K20, 65H10

PII. S1064827597325153

1. Introduction.

In recent years, *optimal flow control* of viscous fluid flows has received considerable attention due to its importance in many applications involving fluid related technology; see, e.g., [3], [10], [11], [12], [14], [15], [16], [17], [18], [19], and [20].

The purpose of this paper is to present some numerically convenient approaches and their implementations to treat optimal Dirichlet control problems associated with the steady Navier–Stokes equations. In finite element approximations of (uncontrolled) boundary value problems for partial differential equations (PDEs), Neumann boundary conditions are generally easier to handle than the Dirichlet ones; the same is true for optimal boundary control problems. Inspired by the penalty method for solving Dirichlet problems for (uncontrolled) elliptic PDEs (see [1]), we proposed in [13] a penalized Neumann control approach for solving the optimal Dirichlet control problem. In [13] we resolved basic mathematical issues such as the convergence of the solutions of the penalized Neumann control problems, the suboptimality of the limit, and the optimality of the limit under further restrictions on the data.

In this paper we will focus on the numerical and computational aspects of the penalized Neumann control approach. The convergence behavior of the penalty approach is demonstrated and its performance is compared with the unpenalized approach. We will consider several test problems with various boundary control set-

*Received by the editors July 29, 1997; accepted for publication (in revised form) April 21, 1998; published electronically May 7, 1999.

http://www.siam.org/journals/sisc/20-5/32515.html

†Department of Mathematics, Iowa State University, Ames, IA 50011-2064 and Department of Mathematics and Statistics, York University, Toronto, Ontario, Canada M3J 1P3 (hou@math.iastate.edu). The work of this author was supported in part by the National Science and Engineering Research Council of Canada.

‡Flow Modeling and Control Branch, NASA Langley Research Center, Mail Stop 170, Hampton, VA 23681 (ravi@fmd00.larc.nasa.gov). The work of this author was supported in part by the Air Force Office of Scientific Research under grants AFOSR F49620-95-1-0447 and AFOSR F49620-95-1-0437 and by NASA under grant NASW-8154.

tings involving velocity tracking and vorticity minimization. These problems are cast as constrained minimization problems for suitable cost functionals subject to the flow equations and boundary controls. The vorticity functional is chosen as $\mathcal{F}(\mathbf{u}) = \int_\Omega |\nabla \times \mathbf{u}|^2 \, d\Omega$, i.e., the L^2-norm of vorticity, and the velocity tracking functional is chosen as $\mathcal{F}(\mathbf{u}) = \int_\Omega |\mathbf{u} - \mathbf{u}_d|^2 \, d\Omega$, i.e., the L^2-distance of the candidate velocity to some desired flow field $\mathbf{u}_d$. Here Ω is the flow domain and the flow is assumed to be stationary. The controls are the boundary velocity field. To solve these constrained minimization problems, we develop a sequential quadratic programming (SQP) method. The SQP method is one of the most popular methods for solving finite-dimensional constrained minimization problems; see, e.g., [2] and [5]. We will use mixed finite element methods to discretize the PDEs that result from the application of the SQP algorithm. Error estimates for the penalty approach will be presented.

It should be noted that the theoretical results of [13] relied on various assumptions on the data or on the functionals. Also, the penalized boundary condition was a nonlinear one. Some of these test examples serve to illustrate that similar results can hold even when some of the assumptions used in [13] are violated or a linear penalized boundary condition is used.

In order to keep the illustration of ideas and computation simple, we restrict our study to cavity and channel domains. For high Reynolds number flows we employ a continuation method on the Reynolds number to globalize the SQP method.

1.1. Description of optimal control problems. The optimal boundary control problem is formulated as follows: Find a triple $(\mathbf{u}, p, \mathbf{g})$ such that the cost functional

$$\mathcal{J}(\mathbf{u}, p, \mathbf{g}) = \mathcal{F}(\mathbf{u}, p) + \frac{\beta^2}{2} \int_\Gamma |\mathbf{g}|^2 \, d\Gamma \tag{1.1}$$

is minimized subject to the steady-state Navier–Stokes equations

$$-\nu \Delta \mathbf{u} + (\mathbf{u} \cdot \nabla)\mathbf{u} + \nabla p = \mathbf{f} \qquad \text{in } \Omega\,, \tag{1.2}$$

$$\nabla \cdot \mathbf{u} = 0 \qquad \text{in } \Omega, \tag{1.3}$$

and

$$\mathbf{u} = \mathbf{g} \qquad \text{on } \Gamma\,. \tag{1.4}$$

Here, Ω is the two-dimensional (bounded) flow domain; Γ is the boundary where control is applied; $\nu > 0$ denotes the constant viscosity; $\mathbf{u}$ and p denote the velocity field and the pressure field, respectively; $\mathbf{f}$ is a prescribed forcing; and $\mathbf{g}$ is the boundary control. In the cost functional $\mathcal{J}$, the term $\mathcal{F}(\mathbf{u}, p)$ is a functional of $(\mathbf{u}, p)$ which unifies the cost functionals described in the previous section and allows for other physical quantities. The appearance of the second term in the cost functional is necessary since we will not impose any a priori constraints on the controls. The parameter β^2 adjusts the relative weight of the two terms in the functional.

We will develop an SQP method to solve the constrained minimization problem (1.1)–(1.4). The partial differential equations that arise in the resulting algorithm are discretized using a finite element method. Numerical results for several prototype examples will be presented.

1.2. Preliminaries. We denote by $L^2(\Omega)$ the collection of square-integrable functions defined on Ω and we denote the associated norm by $\|\cdot\|_0$. Let

$$H^1(\Omega) = \left\{ v \in L^2(\Omega) : \frac{\partial v}{\partial x_i} \in L^2(\Omega) \text{ for } i = 1, 2 \right\},$$
$$H_0^1(\Omega) = \left\{ v \in H^1(\Omega) : v|_\Gamma = 0 \right\},$$
$$\mathbf{L}_n^2(\Gamma) = \left\{ \mathbf{g} \in \mathbf{L}^2(\Gamma) : \int_\Gamma \mathbf{g} \cdot \mathbf{n} d\Gamma = 0 \right\} \quad \text{and} \quad L_0^2(\Omega) = \left\{ q \in L^2(\Omega) : \int_\Omega q \, d\Omega = 0 \right\}.$$

Vector-valued counterparts of these spaces are denoted by boldface symbols, e.g., $\mathbf{H}^1(\Omega) = [H^1(\Omega)]^2$. The trace spaces $H^r(\Gamma)$ $(r > 0)$ are the restriction of $H^{r+1/2}(\Omega)$ to the boundary. We denote the norms and inner products for $H^s(\Omega)$ or $\mathbf{H}^s(\Omega)$ by $\|\cdot\|_s$ and $(\cdot,\cdot)_s$, respectively. The $L^2(\Omega)$ or $\mathbf{L}^2(\Omega)$ inner product is denoted by $(\cdot,\cdot)$. We denote the norms and inner products for $H^r(\Gamma)$ or $\mathbf{H}^r(\Gamma)$ by $\|\cdot\|_{r,\Gamma}$ and $(\cdot,\cdot)_{r,\Gamma}$, respectively. The $L^2(\Gamma)$ or $\mathbf{L}^2(\Gamma)$ inner product is denoted by $(\cdot,\cdot)_\Gamma$.

We define the following standard bilinear and trilinear forms associated with the Navier–Stokes equations:

$$a(\mathbf{u}, \mathbf{v}) = \int_\Omega \nabla \mathbf{u} : \nabla \mathbf{v} \, d\Omega \qquad \forall \, \mathbf{u}, \mathbf{v} \in \mathbf{H}^1(\Omega)$$

(the colon notation stands for the scalar product on $\mathbb{R}^{2\times 2}$),

$$b(\mathbf{u}, q) = -\int_\Omega q \, \nabla \cdot \mathbf{u} \, d\Omega \qquad \forall \, \mathbf{u} \in \mathbf{H}^1(\Omega) \quad \text{and} \quad \forall \, q \in L^2(\Omega),$$

$$c(\mathbf{u}, \mathbf{v}, \mathbf{w}) = \int_\Omega (\mathbf{u} \cdot \nabla)\mathbf{v} \cdot \mathbf{w} \, d\Omega \qquad \forall \, \mathbf{u}, \mathbf{v}, \mathbf{w} \in \mathbf{H}^1(\Omega)$$

and

$$c_1(\mathbf{u}, \mathbf{v}, \mathbf{w}) = \frac{1}{2} \int_\Omega \{(\mathbf{u} \cdot \nabla)\mathbf{v} \cdot \mathbf{w} - (\mathbf{u} \cdot \nabla)\mathbf{w} \cdot \mathbf{v}\} \, d\Omega \qquad \forall \, \mathbf{u}, \mathbf{v}, \mathbf{w} \in \mathbf{H}^1(\Omega).$$

2. Approaches for treating the boundary conditions. From the computational point of view, how one treats the boundary conditions (1.4) can be critical since different treatments of boundary conditions lead to different formulations and computational algorithms. We will, in this section, propose three different treatments and discuss the corresponding formulations of the optimal control problems.

2.1. Approach I. In this approach we introduce the boundary stress as quantity $\mathbf{t}$ to treat the boundary conditions; see [8]. The variational formulation of the problem (1.2)–(1.4) is given as follows: *Find* $\mathbf{u} \in \mathbf{H}^1(\Omega)$, $p \in L_0^2(\Omega)$, *and* $\mathbf{t} \in \mathbf{H}^{-1/2}(\Gamma)$ such that

$$\nu \, a(\mathbf{u}, \mathbf{v}) + c(\mathbf{u}, \mathbf{u}, \mathbf{v}) + b(\mathbf{v}, p) - (\mathbf{v}, \mathbf{t})_\Gamma = (\mathbf{f}, \mathbf{v}) \qquad \forall \, \mathbf{v} \in \mathbf{H}^1(\Omega), \tag{2.1}$$

$$b(\mathbf{u}, q) = 0 \qquad \forall \, q \in L_0^2(\Omega), \tag{2.2}$$

and

$$(\mathbf{u}, \mathbf{s})_\Gamma - (\mathbf{g}, \mathbf{s})_\Gamma = 0 \qquad \forall \, \mathbf{s} \in \mathbf{H}^{-\frac{1}{2}}(\Gamma), \tag{2.3}$$

where $\mathbf{t} = -p\mathbf{n} + \nu\frac{\partial \mathbf{u}}{\partial \mathbf{n}}$. The cost functional is chosen to be of the form

$$\mathcal{J}(\mathbf{u}, p, g) = \mathcal{F}(\mathbf{u}, p) + \frac{\beta^2}{2}\int_\Gamma |\mathbf{g}|^2 \, d\Gamma. \tag{2.4}$$

We define $\mathbf{H}^1_n(\Gamma) = \{\mathbf{z} \in \mathbf{H}^1(\Gamma) : \int_\Gamma \mathbf{z}\cdot\mathbf{n}\, d\Gamma = 0\}$. The precise mathematical statement of the optimal control problem (1.1)–(1.4) can now be given as follows:

(P) Seek a $(\mathbf{u}, p, \mathbf{g}) \in \mathbf{H}^1(\Omega) \times L^2_0(\Omega) \times [\mathbf{H}^{1/2}(\Gamma) \cap \mathbf{L}^2_n(\Gamma)]$ such that (2.4) is minimized subject to the constraints (2.1)–(2.3).

Regarding the existence of an optimal solution, we have the following theorem whose proof is similar to that of [13] (the limit of penalized solutions).

THEOREM 2.1. *Assume that the function $\mathcal{F}(\mathbf{u}, p)$ is convex and lower semicontinuous and there are constants $c_1,\ c_2 \in \mathbb{R}_+$ such that $\mathcal{F}(\mathbf{w}, r) \geq c_1 \|\mathbf{z}\|^2_1 - c_2$ for all $(\mathbf{w}, r) \in \mathbf{H}^1(\Omega) \times L^2_0(\Omega)$ satisfying* (2.1)–(2.3). *Then the minimization problem* (P) *has a solution.*

2.2. Approach II. In this approach we consider a penalized treatment of the boundary conditions. For each $\epsilon \in (0, 1/\nu)$, we consider the following Neumann control problem: Find a $(\mathbf{u}_\epsilon, p_\epsilon, \mathbf{g}_\epsilon) \in \mathbf{H}^1(\Omega) \times L^2(\Omega) \times \mathbf{L}^2(\Gamma)$ such that the functional

$$\mathcal{J}(\mathbf{u}, p, \mathbf{g}) = \mathcal{F}(\mathbf{u}, p) + \frac{\beta^2}{2}\int_\Gamma |\mathbf{g}|^2 \, d\Gamma \tag{2.5}$$

is minimized subject to the steady-state Navier–Stokes equations (1.2)–(1.3) with the nonlinear Neumann (or Robin) type boundary condition

$$-p\mathbf{n} + \nu\frac{\partial \mathbf{u}}{\partial \mathbf{n}} - \frac{1}{2}(\mathbf{u}\cdot\mathbf{n})\mathbf{u} + \frac{1}{\epsilon}\,\mathbf{u} = \frac{1}{\epsilon}\,\mathbf{g} \qquad \text{on } \Gamma\,. \tag{2.6}$$

Formally, we see that as $\epsilon \to 0$, the Neumann boundary condition (2.6) reduces to the Dirichlet boundary condition (1.4) and therefore, we expect that optimal solutions for the Neumann boundary control problems approach an optimal solution for the Dirichlet boundary control problem. Here, ϵ acts as a penalty constant. By formally multiplying (1.2) by a test function $\mathbf{v}$, integrating by parts, and eliminating $-p\mathbf{n}+\nu\frac{\partial \mathbf{u}}{\partial \mathbf{n}}$ in the boundary integrals using (2.6), we obtain

$$\begin{aligned} &\nu a(\mathbf{u}, \mathbf{v}) + \tfrac{1}{\epsilon}(\mathbf{u} - \mathbf{g}, \mathbf{v})_\Gamma - \tfrac{1}{2}((\mathbf{u}\cdot\mathbf{n})\mathbf{u}, \mathbf{v})_\Gamma + c(\mathbf{u}, \mathbf{u}, \mathbf{v}) + b(\mathbf{v}, p) = (\mathbf{f}, \mathbf{v}) \\ &\forall\ \mathbf{v} \in \mathbf{H}^1(\Omega) \end{aligned} \tag{2.7}$$

and

$$b(\mathbf{u}, q) = 0 \qquad \forall\ q \in L^2(\Omega)\,. \tag{2.8}$$

For each $\epsilon > 0$, the penalized optimal Neumann control problems we consider can be stated as follows:

$(\mathrm{P})_\epsilon$ Seek a $(\mathbf{u}_\epsilon, p_\epsilon, \mathbf{g}_\epsilon) \in \mathbf{H}^1(\Omega) \times L^2(\Omega) \times \mathbf{L}^2(\Gamma)$ such that (2.5) is minimized subject to (2.7)–(2.8)\,.

The existence of a solution to $(\mathrm{P})_\epsilon$ is guaranteed by the following theorem in [13].

THEOREM 2.2. *Assume that $\epsilon \in (0, 1/\nu)$ and that the functional $\mathcal{F}(\cdot, \cdot)$ is sequentially weakly lower semicontinuous and bounded below. Then there exists a solution $(\mathbf{u}_\epsilon, p_\epsilon, \mathbf{g}_\epsilon) \in \mathbf{H}^1(\Omega) \times L^2(\Omega) \times \mathbf{L}^2(\Gamma)$ for the optimal control problem* $(\mathrm{P})_\epsilon$.

In order to be able to use solutions of $(\mathrm{P})_\epsilon$ to approximate solutions of (P), we need the following convergence results found in [13]. Having shown the existence of a solution for $(\mathrm{P})_\epsilon$ for each ϵ, we now quote a result from [13] regarding the convergence of $(\mathbf{u}_\epsilon, p_\epsilon, \mathbf{g}_\epsilon)$ as $\epsilon \to 0$.

THEOREM 2.3. *For each $\epsilon \in (0, 1/\nu)$, let $(\mathbf{u}_\epsilon, p_\epsilon, \mathbf{g}_\epsilon) \in \mathbf{H}^1(\Omega) \times L^2(\Omega) \times \mathbf{L}^2(\Gamma)$ be a solution of the optimal Neumann control problem $(\mathrm{P})_\epsilon$ and suppose $\mathcal{F}$ satisfies certain assumptions. Then there exists a $(\widehat{\mathbf{u}}, \widehat{p}, \widehat{\mathbf{g}})$ and a subsequence $\{\epsilon_k\}_{k=1}^{\infty}$ such that as $k \to \infty$,*

$$\mathbf{u}_{\epsilon_k} \rightharpoonup \widehat{\mathbf{u}} \quad \text{in } \mathbf{H}^1(\Omega)\,, \qquad \mathbf{u}_{\epsilon_k} \to \widehat{\mathbf{u}} \quad \text{in } \mathbf{L}^2(\Omega)\,,$$

$$\overline{p_{\epsilon_k}} \rightharpoonup \widehat{p} \quad \text{in } L_0^2(\Omega) \qquad \text{and} \qquad \mathbf{g}_{\epsilon_k} \rightharpoonup \widehat{\mathbf{g}} \quad \text{in } \mathbf{L}^2(\Gamma)\,,$$

where $\overline{p_{\epsilon_k}} = p_{\epsilon_k} - (1/|\Omega|)\int_\Omega p_{\epsilon_k}\, d\Omega$. Furthermore, $(\widehat{\mathbf{u}}, \widehat{p}, \widehat{\mathbf{g}})$ is a suboptimal solution of (P) *in the sense that $\mathcal{J}(\widehat{\mathbf{u}}, \widehat{p}, \widehat{\mathbf{g}}) \le \mathcal{J}(\mathbf{u}, p, \mathbf{g})$ for all $(\mathbf{u}, p, \mathbf{g})$ satisfying* (2.7)–(2.8) *and the regularity condition $-p\mathbf{n} + \frac{\partial \mathbf{u}}{\partial \mathbf{n}} \in \mathbf{L}^2(\Gamma)$.*

If, in addition,

$$\frac{\|\mathbf{f}\|_0}{\nu^2}\sqrt{\frac{1}{\min\{1, \beta^2\}}} < C,$$

where C is a constant depending only on Ω, then $(\widehat{\mathbf{u}}, \widehat{p}, \widehat{\mathbf{g}})$ is a solution of the optimal Dirichlet control problem (P).

Some remarks are in order. First, we did not give here the explicit assumptions on $\mathcal{F}$. But this is not essential since one of the purposes of this present paper is to verify numerically the convergence results when the assumptions are not satisfied. To be precise, those assumptions are satisfied by the vorticity functional but are not satisfied by the tracking functional. The numerical results to be presented indicate that the convergence as $\epsilon \to 0$ is true for both functionals. Second, when problem (P) has a unique solution, the convergence holds for $\epsilon \to 0$ (instead of convergence for a subsequence). Third, using the divergence-free condition of $\mathbf{u}$ and the definition of the antisymmetrized trilinear form $c_1(\cdot,\cdot,\cdot)$, one can verify that (2.7)–(2.8) is equivalent to the system

$$\nu a(\mathbf{u}, \mathbf{v}) + \tfrac{1}{\epsilon}(\mathbf{u} - \mathbf{g}, \mathbf{v})_\Gamma + c_1(\mathbf{u}, \mathbf{u}, \mathbf{v}) + b(\mathbf{v}, p) = (\mathbf{f}, \mathbf{v}) \qquad \forall\, \mathbf{v} \in \mathbf{H}^1(\Omega)$$

and

$$b(\mathbf{u}, q) = 0 \qquad \forall\, q \in L^2(\Omega)\,.$$

Naturally, one is interested in seeing what happens if the trilinear form $c_1(\cdot,\cdot,\cdot)$ is replaced by the trilinear form $c(\cdot,\cdot,\cdot)$. This leads to the next approach.

2.3. Approach III. This approach is very much similar to Approach II except that the Neumann boundary condition is now linear. For each $\epsilon \in (0, 1/\nu)$, we consider the following modified Neumann control problem: Find a $(\mathbf{u}_\epsilon, p_\epsilon, \mathbf{g}_\epsilon) \in \mathbf{H}^1(\Omega) \times L^2(\Omega) \times \mathbf{L}^2(\Gamma)$ such that the functional

$$\mathcal{J}(\mathbf{u}, p, \mathbf{g}) = \mathcal{F}(\mathbf{u}, p) + \frac{\beta^2}{2}\int_\Gamma |\mathbf{g}|^2\, d\Gamma \tag{2.9}$$

is minimized subject to the steady-state Navier–Stokes equations (1.2)–(1.3) with the linear Neumann (or Robin) type boundary condition

$$-p\mathbf{n} + \nu \frac{\partial \mathbf{u}}{\partial \mathbf{n}} + \frac{1}{\epsilon}\,\mathbf{u} = \frac{1}{\epsilon}\,\mathbf{g} \qquad \text{on } \Gamma\,. \tag{2.10}$$

As in the preceding case, we see that as $\epsilon \to 0$, the Neumann boundary condition (2.10) reduces to the Dirichlet boundary condition (1.4) and therefore, we expect that optimal solutions for the Neumann boundary control problems approach an optimal solution for the Dirichlet boundary control problem. By formally multiplying (1.2) by a test function $\mathbf{v}$, integrating by parts, and eliminating $-p\mathbf{n} + \nu \frac{\partial \mathbf{u}}{\partial \mathbf{n}}$ in the boundary integrals using (2.10), we obtain

$$\nu a(\mathbf{u}, \mathbf{v}) + \frac{1}{\epsilon}(\mathbf{u} - \mathbf{g}, \mathbf{v})_\Gamma + c(\mathbf{u}, \mathbf{u}, \mathbf{v}) + b(\mathbf{v}, p) = (\mathbf{f}, \mathbf{v}) \qquad \forall\, \mathbf{v} \in \mathbf{H}^1(\Omega) \tag{2.11}$$

and

$$b(\mathbf{u}, q) = 0 \qquad \forall\, q \in L^2(\Omega)\,. \tag{2.12}$$

For each $\epsilon > 0$, the penalized optimal Neumann control problems we consider can be stated as follows:

$(\mathrm{P}^*)_\epsilon$ Seek a $(\mathbf{u}_\epsilon, p_\epsilon, \mathbf{g}_\epsilon) \in \mathbf{H}^1(\Omega) \times L^2(\Omega) \times \mathbf{L}^2(\Gamma)$ such that (2.9) is minimized subject to (2.11)–(2.12).

Results similar to those of Theorems 2.1–2.3 for $(\mathrm{P})_\epsilon$ can also be obtained for $(\mathrm{P}^*)_\epsilon$ by adopting the arguments made in [13] for those theorems.

3. SQP methods for optimal control problems. In this section we develop numerical algorithms for solving the steady-state optimal control problem described in section 1.1. We will first present an SQP method to solve the constrained minimization problem (1.1)–(1.4). The SQP method solves the nonlinear optimal control problem (1.1)–(1.4) by a sequence of linear quadratic control problems. In other words, SQP requires satisfaction of only a linear approximation of the state constraints, avoiding the need to converge fully. Thus, the state equations are satisfied as the control values converge to their optimal values. This is in contrast to gradient based methods which require satisfaction of the state equations at each iteration which can be very unfavorable especially for those problems governed by the Navier–Stokes equations.

3.1. SQP method for (P). In order to precisely define the SQP method for (P), let us introduce some notation. In the following we will denote the current iterate by $(\mathbf{v}^c, \boldsymbol{\lambda}^c) = (\mathbf{u}^c, p^c, \mathbf{t}^c, \boldsymbol{\mu}^c, \pi^c, \boldsymbol{\tau}^c, \mathbf{g}^c)$, the new iterate by $(\mathbf{v}^+, \boldsymbol{\lambda}^+) = (\mathbf{u}^+, p^+, \mathbf{t}^+, \boldsymbol{\mu}^+, \pi^+, \boldsymbol{\tau}^+, \mathbf{g}^+)$, the Lagrangian $\mathcal{L}$ by

$$\begin{aligned}\mathcal{L}(\mathbf{u}, p, \mathbf{t}, \mathbf{g}, \boldsymbol{\mu}, \pi, \boldsymbol{\tau}) &= \mathcal{J}(\mathbf{u}, p, \mathbf{g}) - \nu a(\mathbf{u}, \boldsymbol{\mu}) + (\boldsymbol{\mu}, \mathbf{t})_\Gamma - c(\mathbf{u}, \mathbf{u}, \boldsymbol{\mu}) - b(\boldsymbol{\mu}, p) \\ &\quad + (\mathbf{f}, \boldsymbol{\mu}) - b(\mathbf{u}, \pi) - (\mathbf{u}, \boldsymbol{\tau})_\Gamma + (\mathbf{g}, \boldsymbol{\tau})_\Gamma \qquad \forall\, (\mathbf{u}, p, \mathbf{t}, \mathbf{g}, \boldsymbol{\mu}, \pi, \boldsymbol{\tau})\,,\end{aligned} \tag{3.1}$$

and their first and second derivatives, respectively, by

$$\mathcal{L}_{\mathbf{v}}(\mathbf{v}^c, \boldsymbol{\lambda}^c)[\mathbf{d}], \qquad \mathcal{L}_{\mathbf{vv}}(\mathbf{v}^c, \boldsymbol{\lambda}^c)[\mathbf{d}, \mathbf{d}],$$

where $\mathbf{d} = \mathbf{v} - \mathbf{v}^c$ is the search direction. In the SQP method the new iterate is computed as the solution of the following minimization problem:

$$\mathrm{Min}\left\{ \mathcal{L}_{\mathbf{v}}(\mathbf{v}^c)[\mathbf{d}] + \frac{1}{2}\mathcal{L}_{\mathbf{vv}}(\mathbf{v}^c, \boldsymbol{\lambda}^c)[\mathbf{d}, \mathbf{d}] \right\} \tag{3.2}$$

subject to the linearized state equations

$$\begin{aligned}\nu\, a(\mathbf{u},\mathbf{v}) + c(\mathbf{u}^c,\mathbf{u},\mathbf{v}) + c(\mathbf{u},\mathbf{u}^c,\mathbf{v}) + b(\mathbf{v},p) - (\mathbf{v},\mathbf{t})_\Gamma \\ = (\mathbf{f},\mathbf{v}) + c(\mathbf{u}^c,\mathbf{u}^c,\mathbf{v}) \qquad \forall\, \mathbf{v}\in \mathbf{H}^1(\Omega)\,,\end{aligned} \tag{3.3}$$

$$b(\mathbf{u},q) = 0 \qquad \forall\, q\in L_0^2(\Omega), \tag{3.4}$$

and

$$(\mathbf{u},\mathbf{s})_\Gamma - (\mathbf{g},\mathbf{s})_\Gamma = 0 \quad \forall\, \mathbf{s}\in \mathbf{H}^{-\frac{1}{2}}(\Gamma)\,. \tag{3.5}$$

Thus the SQP method forms the following iterative method, given initial estimates $\mathbf{v}^{(1)}$ and $\boldsymbol{\lambda}^{(1)}$.

ALGORITHM A1 (SQP method for (P)). *For $k = 1, 2, \ldots$:*

Step 1. *Solve* (3.3)–(3.5) *to determine* $\mathbf{d}^{(k)}$ *and let* $\boldsymbol{\lambda}^{(k+1)}$ *be the Lagrange multipliers of the linear constraints* (3.2)–(3.5).

Step 2. *Set* $\mathbf{v}^{(k+1)} = \mathbf{v}^{(k)} + \eta^{(k)}\mathbf{d}^{(k)}$.

The parameter η in the algorithm is the step length which has to be computed by line search (see [2]) in order to globalize the algorithm. When the current iterate is inside the contraction ball, one can set $\eta = 1$ for all the successive iterations. However, we will propose a simple alternative approach for globalization for the class of flow control problems studied in this article which is based on continuation on the Reynolds number.

The execution of Step 2, that is, a solution to the linear quadratic subproblem (3.2)–(3.5), is obtained by solving the following necessary conditions of optimality:

$$\mathcal{L}^s_{\mathbf{v}} = 0, \quad \mathcal{L}^s_{\boldsymbol{\lambda}} = 0, \quad \mathcal{L}^s_{\mathbf{g}} = 0\,,$$

where $\mathcal{L}^s$ is the Lagrangian corresponding to the linear quadratic subproblem. Thus, given the current iterate $(\mathbf{v}^c, \boldsymbol{\lambda}^c)$, one obtains the new iterate $(\mathbf{v}^+, \boldsymbol{\lambda}^+)$ by solving the following PDEs:

$$(S)\quad \begin{cases} \nu\, a(\mathbf{u},\mathbf{v}) + c(\mathbf{u}^c,\mathbf{u},\mathbf{v}) + c(\mathbf{u},\mathbf{u}^c,\mathbf{v}) + b(p,\mathbf{v}) - (\mathbf{v},\mathbf{t})_\Gamma \\ \qquad = (\mathbf{f},\mathbf{v}) + c(\mathbf{u}^c,\mathbf{u}^c,\mathbf{v}) \qquad \forall\, \mathbf{v}\in \mathbf{H}^1(\Omega)\,, \\ b(\mathbf{u},q) = 0 \qquad \forall\, q\in L_0^2(\Omega)\,, \\ (\mathbf{u},\mathbf{s})_\Gamma - (\mathbf{g},\mathbf{s})_\Gamma = 0 \quad \forall\, \mathbf{s}\in \mathbf{H}^{-\frac{1}{2}}(\Gamma)\,, \\ \nu a(\boldsymbol{\mu},\mathbf{w}) + c(\mathbf{u}^c,\mathbf{w},\boldsymbol{\mu}-\boldsymbol{\mu}^c) + c(\mathbf{w},\mathbf{u}^c,\boldsymbol{\mu}-\boldsymbol{\mu}^c) + b(\mathbf{w},\pi) \\ \qquad -(\mathbf{w},\boldsymbol{\tau})_\Gamma + c(\mathbf{u},\mathbf{w},\boldsymbol{\mu}^c) + c(\mathbf{w},\mathbf{u},\boldsymbol{\mu}^c) \\ \qquad = \langle \mathcal{F}_{\mathbf{u}}(\mathbf{u}^c),\mathbf{w}\rangle + \langle \mathcal{F}_{\mathbf{uu}}(\mathbf{u}^c)(\mathbf{u}-\mathbf{u}^c),\mathbf{w}\rangle \quad \forall\, \mathbf{w}\in \mathbf{H}^1(\Omega)\,, \\ b(\boldsymbol{\mu},r) = \langle \mathcal{F}_p, r\rangle + \langle \mathcal{F}_{pp}(p-p^c), r\rangle \qquad \forall\, r\in L_0^2(\Omega)\,, \\ (\boldsymbol{\mu},\mathbf{y})_\Gamma = 0 \qquad \forall\, \mathbf{y}\in \mathbf{H}^{-\frac{1}{2}}(\Gamma)\,, \\ \beta^2(\mathbf{g},\mathbf{k})_\Gamma = -(\mathbf{k},\boldsymbol{\tau})_\Gamma \quad \forall\, \mathbf{k}\in \mathbf{L}^2_n(\Gamma). \end{cases}$$

We note here that for each fixed $\boldsymbol{\tau}$, the last equation in (S) is equivalent to finding a $\mathbf{g} \in \mathbf{L}^2(\Gamma)$

$$\beta^2(\mathbf{g},\mathbf{k})_\Gamma + \gamma \int_\Gamma \mathbf{k}\cdot\mathbf{n} d\Gamma = -(\mathbf{k},\boldsymbol{\tau})_\Gamma \quad \forall\, \mathbf{k} \in \mathbf{L}^2(\Gamma) \tag{3.6}$$

and

$$\int_\Gamma \mathbf{g}\cdot\mathbf{n} d\Gamma = 0, \tag{3.7}$$

for $\mathbf{g} \in \mathbf{H}^1(\Gamma)$, where $\gamma \in \mathbb{R}$ is an additional constant that accounts for the constraint (3.7). Although the last equations in (S) and (3.6)–(3.7) are equivalent, the latter is used in our computations since it can be easily discretized.

3.2. SQP method for $(\mathrm{P})_\epsilon$. The SQP method for the problem $(\mathrm{P})_\epsilon$ is defined similarly. In fact, one redefines the Lagrangian $\mathcal{L}$ by

$$\begin{aligned}\mathcal{L}(\mathbf{u},p,\mathbf{g},\boldsymbol{\mu},\pi) &= \mathcal{J}(\mathbf{u},p,\mathbf{g}) - \nu a(\mathbf{u},\boldsymbol{\mu}) - \tfrac{1}{\epsilon}(\mathbf{u},\boldsymbol{\mu})_\Gamma + \tfrac{1}{2}((\mathbf{u}\cdot\mathbf{n})\mathbf{u},\boldsymbol{\mu})_\Gamma \\ &\quad -c(\mathbf{u},\mathbf{u},\boldsymbol{\mu}) - b(\boldsymbol{\mu},p) + \tfrac{1}{\epsilon}(\mathbf{g},\boldsymbol{\mu})_\Gamma - b(\mathbf{u},\pi) + (\mathbf{f},\boldsymbol{\mu}) \qquad \forall\, (\mathbf{u},p,\mathbf{g},\boldsymbol{\mu},\pi)\,.\end{aligned} \tag{3.8}$$

Then the new iterate is computed as the solution of the following minimization problem:

$$\mathrm{Min}\left\{\mathcal{L}_{\mathbf{v}}(\mathbf{v}^c)[\mathbf{d}] + \frac{1}{2}\mathcal{L}_{\mathbf{vv}}(\mathbf{v}^c,\boldsymbol{\lambda}^c)[\mathbf{d},\mathbf{d}]\right\} \tag{3.9}$$

subject to the linearized state equations

$$\begin{aligned}&\nu a(\mathbf{u},\mathbf{v}) + \tfrac{1}{\epsilon}(\mathbf{u}-\mathbf{g},\mathbf{v})_\Gamma - \tfrac{1}{2}((\mathbf{u}\cdot\mathbf{n})\mathbf{u}^c,\mathbf{v})_\Gamma - \tfrac{1}{2}((\mathbf{u}^c\cdot\mathbf{n})\mathbf{u},\mathbf{v})_\Gamma + c(\mathbf{u}^c,\mathbf{u},\mathbf{v}) \\ &\qquad +c(\mathbf{u},\mathbf{u}^c,\mathbf{v}) + b(\mathbf{v},p) = (\mathbf{f},\mathbf{v}) + c(\mathbf{u}^c,\mathbf{u}^c,\mathbf{v}) - \tfrac{1}{2}((\mathbf{u}^c\cdot\mathbf{n})\mathbf{u}^c,\mathbf{v})_\Gamma \quad \forall\, \mathbf{v} \in \mathbf{H}^1(\Omega)\end{aligned} \tag{3.10}$$

and

$$b(\mathbf{u},q) = 0 \qquad \forall\, q \in L_0^2(\Omega)\,. \tag{3.11}$$

By modifying Algorithm A1 we obtain an algorithm for solving $(\mathrm{P})_\epsilon$ given initial estimates $\mathbf{v}^{(1)}$ and $\boldsymbol{\lambda}^{(1)}$.

Algorithm A2 (SQP method for $(\mathrm{P})_\epsilon$). *For $k = 1, 2, \ldots$:*

Step 1. *Solve* (3.9)–(3.11) *to determine* $\mathbf{d}^{(k)}$ *and let* $\boldsymbol{\lambda}^{(k+1)}$ *be the Lagrange multipliers of the linear constraints* (3.2)–(3.11).

Step 2. *Set* $\mathbf{v}^{(k+1)} = \mathbf{v}^{(k)} + \eta^{(k)}\mathbf{d}^{(k)}$.

Step 2 is carried out as follows. Given the current iterate $(\mathbf{v}^c,\boldsymbol{\lambda}^c)$, one obtains

the new iterate $(\mathbf{v}^+, \boldsymbol{\lambda}^+)$ by solving the following PDEs:

$$(S)_\epsilon \quad \begin{cases} \nu\, a(\mathbf{u},\mathbf{v}) + c(\mathbf{u}^c,\mathbf{u},\mathbf{v}) + c(\mathbf{u},\mathbf{u}^c,\mathbf{v}) + b(\mathbf{v},p) + \frac{1}{\epsilon}(\mathbf{u}-\mathbf{g},\mathbf{v})_\Gamma \\ \qquad -\frac{1}{2}((\mathbf{u}\cdot\mathbf{n})\mathbf{u}^c,\mathbf{v})_\Gamma - \frac{1}{2}((\mathbf{u}^c\cdot\mathbf{n})\mathbf{u},\mathbf{v})_\Gamma \\ \qquad = (\mathbf{f},\mathbf{v}) + c(\mathbf{u}^c,\mathbf{u}^c,\mathbf{v}) - \frac{1}{2}((\mathbf{u}^c\cdot\mathbf{n})\mathbf{u}^c,\mathbf{v})_\Gamma \qquad \forall\, \mathbf{v}\in\mathbf{H}^1(\Omega)\,, \\ b(\mathbf{u},q) = 0 \qquad \forall\, q\in L^2(\Omega)\,, \\ \nu a(\boldsymbol{\mu},\mathbf{w}) + c(\mathbf{u}^c,\mathbf{w},\boldsymbol{\mu}-\boldsymbol{\mu}^c) + c(\mathbf{w},\mathbf{u}^c,\boldsymbol{\mu}-\boldsymbol{\mu}^c) + c(\mathbf{u},\mathbf{w},\boldsymbol{\mu}^c) + c(\mathbf{w},\mathbf{u},\boldsymbol{\mu}^c) \\ \qquad +b(\mathbf{w},\pi) + \frac{1}{\epsilon}(\boldsymbol{\mu},\mathbf{w})_\Gamma - \frac{1}{2}((\mathbf{w}\cdot\mathbf{n})\mathbf{u},\boldsymbol{\mu}^c)_\Gamma - \frac{1}{2}((\mathbf{u}^c\cdot\mathbf{n})\mathbf{w},\boldsymbol{\mu}-\boldsymbol{\mu}^c)_\Gamma \\ \qquad -\frac{1}{2}((\mathbf{w}\cdot\mathbf{n})\mathbf{u}^c,\boldsymbol{\mu}-\boldsymbol{\mu}^c)_\Gamma - \frac{1}{2}((\mathbf{u}\cdot\mathbf{n})\mathbf{w},\boldsymbol{\mu}^c)_\Gamma \\ \qquad = \langle \mathcal{F}_{\mathbf{u}}(\mathbf{u}^c),\mathbf{w}\rangle + \langle \mathcal{F}_{\mathbf{uu}}(\mathbf{u}^c)(\mathbf{u}-\mathbf{u}^c),\mathbf{w}\rangle \quad \forall\, \mathbf{w}\in\mathbf{H}^1(\Omega)\,, \\ b(\boldsymbol{\mu},r) = \langle \mathcal{F}_p(p^c),r\rangle + \langle \mathcal{F}_{pp}(p^c)(p-p^c),r\rangle \qquad \forall\, r\in L^2(\Omega)\,, \\ \beta^2(\mathbf{g},\mathbf{z})_\Gamma + \frac{1}{\epsilon}(\boldsymbol{\mu},\mathbf{z})_\Gamma = 0 \quad \forall\, \mathbf{z}\in\mathbf{L}^2(\Gamma) \end{cases}$$

3.3. SQP method for $(\mathbf{P^*})_\epsilon$. The SQP method for the problem $(\mathrm{P}^*)_\epsilon$ can be defined similarly. In fact, one redefines the Lagrangian $\mathcal{L}$ by

$$\begin{aligned} \mathcal{L}(\mathbf{u},p,\mathbf{g},\boldsymbol{\mu},\pi) &= \mathcal{J}(\mathbf{u},p,\mathbf{g}) - \nu a(\mathbf{u},\boldsymbol{\mu}) - \tfrac{1}{\epsilon}(\mathbf{u},\boldsymbol{\mu})_\Gamma - c(\mathbf{u},\mathbf{u},\boldsymbol{\mu}) \\ &\quad -b(\boldsymbol{\mu},p) + \tfrac{1}{\epsilon}(\mathbf{g},\boldsymbol{\mu})_\Gamma - b(\mathbf{u},\pi) + (\mathbf{f},\boldsymbol{\mu}) \qquad \forall\, (\mathbf{u},p,\mathbf{g},\boldsymbol{\mu},\pi)\,. \end{aligned} \tag{3.12}$$

Then the new iterate is computed as the solution of the following minimization problem:

$$\mathrm{Min}\left\{ \mathcal{L}_{\mathbf{v}}(\mathbf{v}^c)[\mathbf{d}] + \frac{1}{2}\mathcal{L}_{\mathbf{vv}}(\mathbf{v}^c,\boldsymbol{\lambda}^c)[\mathbf{d},\mathbf{d}] \right\} \tag{3.13}$$

subject to the linearized state equations

$$\begin{aligned} &\nu a(\mathbf{u},\mathbf{v}) + \tfrac{1}{\epsilon}(\mathbf{u}-\mathbf{g},\mathbf{v})_\Gamma + c_1(\mathbf{u}^c,\mathbf{u},\mathbf{v}) + c_1(\mathbf{u},\mathbf{u}^c,\mathbf{v}) + b(\mathbf{v},p) \\ &\qquad = (\mathbf{f},\mathbf{v}) + c_1(\mathbf{u}^c,\mathbf{u}^c,\mathbf{v}) \qquad \forall\, \mathbf{v}\in\mathbf{H}^1(\Omega) \end{aligned} \tag{3.14}$$

and

$$b(\mathbf{u},q) = 0 \qquad \forall\, q\in L^2_0(\Omega)\,. \tag{3.15}$$

Algorithm A1 also needs to be modified to obtain an algorithm for $(\mathrm{P}^*)_\epsilon$ given initial estimates $\mathbf{v}^{(1)}$ and $\boldsymbol{\lambda}^{(1)}$.

ALGORITHM A3 (SQP method $(\mathrm{P}^*)_\epsilon$). *For $k = 1, 2, \ldots$:*

Step 1. *Solve* (3.13)–(3.15) *to determine* $\mathbf{d}^{(k)}$ *and let* $\boldsymbol{\lambda}^{(k+1)}$ *be the Lagrange multipliers of the linear constraints* (3.14)–(3.15).

Step 2. *Set* $\mathbf{v}^{(k+1)} = \mathbf{v}^{(k)} + \eta^{(k)}\mathbf{d}^{(k)}$.

Step 2 is carried out as follows. Given the current iterate $(\mathbf{v}^c, \boldsymbol{\lambda}^c)$, one obtains the new iterate $(\mathbf{v}^+, \boldsymbol{\lambda}^+)$ by solving the following PDEs:

$$(S^*)_\epsilon \begin{cases} \nu\, a(\mathbf{u},\mathbf{v}) + c_1(\mathbf{u}^c,\mathbf{u},\mathbf{v}) + c_1(\mathbf{u},\mathbf{u}^c,\mathbf{v}) + b(\mathbf{v},p) + \frac{1}{\epsilon}(\mathbf{u}-\mathbf{g},\mathbf{v})_\Gamma \\ \qquad = (\mathbf{f},\mathbf{v}) + c_1(\mathbf{u}^c,\mathbf{u}^c,\mathbf{v}) \qquad \forall\, \mathbf{v} \in \mathbf{H}^1(\Omega)\,, \\ b(\mathbf{u},q) = 0 \qquad \forall\, q \in L^2(\Omega)\,, \\ \nu a(\boldsymbol{\mu},\mathbf{w}) + c_1(\mathbf{u}^c,\mathbf{w},\boldsymbol{\mu}-\boldsymbol{\mu}^c) + c_1(\mathbf{w},\mathbf{u}^c,\boldsymbol{\mu}-\boldsymbol{\mu}^c) + b(\mathbf{w},\pi) + c_1(\mathbf{u},\mathbf{w},\boldsymbol{\mu}^c) \\ \qquad + c_1(\mathbf{w},\mathbf{u},\boldsymbol{\mu}^c) + \frac{1}{\epsilon}(\boldsymbol{\mu},\mathbf{w})_\Gamma \\ \qquad = \langle \mathcal{F}_{\mathbf{u}}(\mathbf{u}^c),\mathbf{w}\rangle + \langle \mathcal{F}_{\mathbf{uu}}(\mathbf{u}^c)(\mathbf{u}-\mathbf{u}^c),\mathbf{w}\rangle \quad \forall\, \mathbf{w} \in \mathbf{H}^1(\Omega)\,, \\ b(\boldsymbol{\mu},r) = \langle \mathcal{F}_p(p^c),r\rangle + \langle \mathcal{F}_{pp}(p^c)(p-p^c),\mathbf{w}\rangle \qquad \forall\, r \in L^2(\Omega)\,, \\ \beta^2(\mathbf{g},\mathbf{z})_\Gamma + \frac{1}{\epsilon}(\boldsymbol{\mu},\mathbf{z})_\Gamma = 0 \quad \forall\, \mathbf{z} \in \mathbf{L}^2(\Gamma). \end{cases}$$

The SQP methods discussed here display quadratic convergence when the optimal solutions are away from the limit and bifurcations points and when the initial iterate $(\mathbf{v}^{(0)}, \boldsymbol{\lambda}^{(0)})$ is sufficiently close to the optimal solution.

4. Finite element approximation and implementation issues. In this section, we will describe finite element algorithms to discretize the systems (S), $(S)_\epsilon$, and $(S^*)_\epsilon$. Each of those systems consists of Navier–Stokes equations for the variables $\mathbf{u}$ and p, and PDEs, which are very similar in character to the Navier–Stokes equations, for the Lagrange multipliers (adjoint variables) $\boldsymbol{\mu}$ and π. Therefore when one designs algorithms for the above mentioned systems, the knowledge and insights gained in designing algorithms for the Navier–Stokes equations should be utilized. One of the difficulties encountered in the computation of the Navier–Stokes equations lies in computing pressure in a stable manner. In the computation of systems (S), $(S)_\epsilon$, and $(S^*)_\epsilon$, one should expect the same difficulty for both pressure p and Lagrange multiplier π. Thus the finite element spaces for the unknowns involved have to be chosen judiciously. Precisely, the finite element pairs for $\mathbf{u}$ and p and those for $\boldsymbol{\mu}$ and π have to satisfy the inf-sup condition; see, e.g., [7], [8], and [9] for details. The errors for finite element approximations of solutions of (S), $(S)_\epsilon$, and $(S^*)_\epsilon$ can be analyzed by first deriving the error estimates of a suitably chosen principal linear part and then fitting the systems in question into the framework of Brezzi–Rappaz–Raviart theory; see [6]. We will give the detailed derivation of error estimates for the case of $(S^*)_\epsilon$ and will simply comment on the cases of (S) and $(S)_\epsilon$.

For simplicity, we specialize $(S^*)_\epsilon$ to the case where the functional $\mathcal{F}(\mathbf{u},p) = \mathcal{F}(\mathbf{u})$ so that $\boldsymbol{\mu}$ satisfies the divergence-free condition. The finite element approximation of $(S^*)_\epsilon$ can be defined as follows: First, we choose finite element spaces $\mathbf{V}_h \subset \mathbf{H}^1(\Omega)$ and $M_h \subset L^2(\Omega)$ satisfying the properties

$$\inf_{\mathbf{v}_h \in \mathbf{V}_h} \|\mathbf{v}-\mathbf{v}_h\|_1 \le Ch^m \|\mathbf{v}\|_{m+1} \qquad \forall\, \mathbf{v} \in \mathbf{H}^{m+1}(\Omega),\ 1 \le m \le k,$$

$$\inf_{q_h \in M_h} \|q-q_h\|_0 \le Ch^m \|q\|_m \qquad 1 \le m \le k \quad (k \text{ is a positive integer}),$$

and

$$\inf_{q_h\in M_h}\sup_{\mathbf{v}_h\in\mathbf{V}_h}\frac{b(\mathbf{v}_h,q_h)}{\|\mathbf{v}_h\|_1\,\|q_h\|_0}\geq C,\qquad \text{where } C \text{ is independent of } h;$$

then we seek a $(\mathbf{u}_h,p_h,\mathbf{g}_h,\boldsymbol{\mu}_h,\pi_h)\in\mathbf{V}_h\times M_h\times\mathbf{V}_h\big|_\Gamma\times\mathbf{V}_h\times M_h$ such that

$$(\mathrm{S}_h^*)_\epsilon\quad\begin{cases}\nu\,a(\mathbf{u}_h,\mathbf{v}_h)+c(\mathbf{u}_h^c,\mathbf{u}_h,\mathbf{v}_h)+c(\mathbf{u}_h,\mathbf{u}_h^c,\mathbf{v}_h)+\frac{1}{\epsilon}(\mathbf{u}_h-\mathbf{g}_h,\mathbf{v}_h)_\Gamma\\ \qquad +b(\mathbf{v}_h,p_h)=(\mathbf{f},\mathbf{v}_h)+c(\mathbf{u}_h^c,\mathbf{u}_h^c,\mathbf{v}_h)\qquad\forall\,\mathbf{v}_h\in\mathbf{V}_h\,,\\ b(\mathbf{u}_h,q_h)=0\qquad\forall\,q_h\in M_h\,,\\ \nu\,a(\boldsymbol{\mu}_h,\mathbf{w}_h)+c(\mathbf{u}_h^c,\mathbf{w}_h,\boldsymbol{\mu}_h-\boldsymbol{\mu}_h^c)+c(\mathbf{w}_h,\mathbf{u}_h^c,\boldsymbol{\mu}_h-\boldsymbol{\mu}_h^c)+b(\mathbf{w}_h,\pi_h)\\ \qquad +c(\mathbf{u}_h,\mathbf{w}_h,\boldsymbol{\mu}_h^c)+c(\mathbf{w}_h,\mathbf{u}_h,\boldsymbol{\mu}_h^c)+\frac{1}{\epsilon}(\boldsymbol{\mu}_h,\mathbf{w}_h)_\Gamma\\ \qquad =\langle\mathcal{F}_{\mathbf{u}}(\mathbf{u}_h^c),\mathbf{w}_h\rangle+\langle\mathcal{F}_{\mathbf{uu}}(\mathbf{u}_h^c)(\mathbf{u}_h-\mathbf{u}_h^c),\mathbf{w}_h\rangle\qquad\forall\,\mathbf{w}_h\in\mathbf{V}_h\,,\\ b(\boldsymbol{\mu}_h,r_h)=0\qquad\forall\,r_h\in M_h\,,\\ \beta^2(\mathbf{g}_h,\mathbf{z}_h)_\Gamma+\frac{1}{\epsilon}(\boldsymbol{\mu}_h,\mathbf{z}_h)_\Gamma=0\qquad\forall\,\mathbf{z}_h\in\mathbf{V}_h\big|_\Gamma\,.\end{cases}$$

We treat the control variables $\mathbf{g}$ in $(\mathrm{S}^*)_\epsilon$ and $\mathbf{g}_h$ in $(\mathrm{S}_h^*)_\epsilon$ as auxiliary variables and regard, respectively, $(\mathrm{S}^*)_\epsilon$ as a system for $(\mathbf{u},p,\boldsymbol{\mu},\pi)$ and $(\mathrm{S}_h^*)_\epsilon$ as a system for $(\mathbf{u}_h,p_h,\boldsymbol{\mu}_h,\pi_h)$. Now, we choose the principal linear part for $(\mathrm{S}^*)_\epsilon$ as

$$\begin{cases}\nu\,a(\tilde{\mathbf{u}},\mathbf{v})+b(\mathbf{v},\tilde{p})+\frac{1}{\epsilon}(\tilde{\mathbf{u}}-\tilde{\mathbf{g}},\mathbf{v})_\Gamma=(\boldsymbol{\phi},\mathbf{v})\qquad\forall\,\mathbf{v}\in\mathbf{H}^1(\Omega)\,,\\ b(\tilde{\mathbf{u}},q)=0\qquad\forall\,q\in L^2(\Omega)\,,\\ \nu a(\tilde{\boldsymbol{\mu}},\mathbf{w})+b(\mathbf{w},\tilde{\pi})+\frac{1}{\epsilon}(\tilde{\boldsymbol{\mu}},\mathbf{w})_\Gamma=\langle\boldsymbol{\psi},\mathbf{w}\rangle\qquad\forall\,\mathbf{w}\in\mathbf{H}^1(\Omega)\,,\\ b(\tilde{\boldsymbol{\mu}},r)=0\qquad\forall\,r\in L^2(\Omega)\,,\\ \beta^2(\tilde{\mathbf{g}},\mathbf{z})_\Gamma+\frac{1}{\epsilon}(\tilde{\boldsymbol{\mu}},\mathbf{z})_\Gamma=0\qquad\forall\,\mathbf{z}\in\mathbf{L}^2(\Gamma)\,.\end{cases}$$

We denote the solution operator of this system by T, i.e., $(\tilde{\mathbf{u}},\tilde{p},\tilde{\boldsymbol{\mu}},\tilde{\pi})=T(\boldsymbol{\phi},\boldsymbol{\psi})$. Similarly, we can define the approximate principal linear operator T_h as the solution operator for the linear finite element system

$$\begin{cases}\nu\,a(\tilde{\mathbf{u}}_h,\mathbf{v}_h)+b(\mathbf{v}_h,\tilde{p}_h)+\frac{1}{\epsilon}(\tilde{\mathbf{u}}_h-\tilde{\mathbf{g}}_h,\mathbf{v}_h)_\Gamma=(\boldsymbol{\phi},\mathbf{v}_h)\qquad\forall\,\mathbf{v}_h\in\mathbf{V}_h\,,\\ b(\tilde{\mathbf{u}}_h,q_h)=0\qquad\forall\,q_h\in M_h\,,\\ \nu a(\tilde{\boldsymbol{\mu}}_h,\mathbf{w}_h)+b(\mathbf{w}_h,\tilde{\pi}_h)+\frac{1}{\epsilon}(\tilde{\boldsymbol{\mu}}_h,\mathbf{w}_h)_\Gamma=\langle\boldsymbol{\psi},\mathbf{w}_h\rangle\qquad\forall\,\mathbf{w}_h\in\mathbf{V}_h\,,\\ b(\tilde{\boldsymbol{\mu}}_h,r_h)=0\qquad\forall\,r_h\in M_h\,,\\ \beta^2(\tilde{\mathbf{g}}_h,\mathbf{z}_h)_\Gamma+\frac{1}{\epsilon}(\tilde{\boldsymbol{\mu}}_h,\mathbf{z}_h)_\Gamma=0\qquad\forall\,\mathbf{z}_h\in\mathbf{V}_h\big|_\Gamma\,,\end{cases}$$

i.e., $(\tilde{\mathbf{u}}_h,\tilde{p}_h,\tilde{\boldsymbol{\mu}}_h,\tilde{\pi}_h)=T_h(\boldsymbol{\phi},\boldsymbol{\psi})$. We have the following error estimate for the approximation of the principal linear part.

LEMMA 4.1. *Let* $(\tilde{\mathbf{u}}, \tilde{p}, \tilde{\boldsymbol{\mu}}, \tilde{\pi})$ *and* $(\tilde{\mathbf{u}}_h, \tilde{p}_h, \tilde{\boldsymbol{\mu}}_h, \tilde{\pi}_h)$ *be the solution of the linear systems defined above. Then*

$$\begin{aligned} &\|\tilde{\mathbf{u}} - \tilde{\mathbf{u}}_h\|_1 + \|\tilde{p} - \tilde{p}_h\|_0 + \|\tilde{\boldsymbol{\mu}} - \tilde{\boldsymbol{\mu}}_h\|_1 + \|\tilde{\pi} - \tilde{\pi}_h\|_0 \\ &\leq Ch^m(\|\tilde{\mathbf{u}}\|_{m+1} + \|\tilde{p}\|_m + \|\tilde{\boldsymbol{\mu}}\|_{m+1} + \|\tilde{\pi}\|_m). \end{aligned} \tag{4.1}$$

Proof. The proof of this result makes use of the techniques in the proof of an abstract approximation result of [6, Thm. II.1.1, pp. 114–116]. We will only sketch the main steps. From the equations involving $(\tilde{\boldsymbol{\mu}}, \tilde{\pi})$ and $(\tilde{\boldsymbol{\mu}}_h, \tilde{\pi}_h)$ we obtain

$$\begin{aligned} &\|\nabla\tilde{\boldsymbol{\mu}} - \nabla\tilde{\boldsymbol{\mu}}_h\|_0 + \tfrac{1}{\sqrt{\epsilon}}\|\tilde{\boldsymbol{\mu}} - \tilde{\boldsymbol{\mu}}_h\|_{0,\Gamma} \\ &\leq \|\nabla\tilde{\boldsymbol{\mu}} - \nabla\boldsymbol{\zeta}_h\|_0 + \tfrac{1}{\sqrt{\epsilon}}\|\tilde{\boldsymbol{\mu}} - \boldsymbol{\zeta}_h\|_{0,\Gamma} + C\|\tilde{\pi} - \lambda_h\|_0 \qquad \forall\, \boldsymbol{\zeta}_h \in \mathbf{Z}_h,\ \forall\, \lambda_h \in M_h, \end{aligned}$$

where $\mathbf{Z}_h \equiv \{\mathbf{v}_h \in \mathbf{V}_h : b(\mathbf{v}_h, q_h) = 0, \forall\ q_h \in M_h\}$. Using the inf-sup condition we deduce

$$\inf_{\boldsymbol{\zeta}_h \in \mathbf{Z}_h} \|\tilde{\boldsymbol{\mu}} - \boldsymbol{\zeta}_h\|_1 \leq C \inf_{\boldsymbol{\omega}_h \in \mathbf{V}_h} \|\tilde{\boldsymbol{\mu}} - \boldsymbol{\omega}_h\|_1$$

so that combining with the previous estimate and the fact that $\|\tilde{\boldsymbol{\mu}} - \boldsymbol{\omega}_h\|_{0,\Gamma} \leq Ch^{1/2}\|\tilde{\boldsymbol{\mu}} - \boldsymbol{\omega}_h\|_1$ (see [8]), we are led to

$$\begin{aligned} &\|\nabla\tilde{\boldsymbol{\mu}} - \nabla\tilde{\boldsymbol{\mu}}_h\|_0 + \tfrac{1}{\sqrt{\epsilon}}\|\tilde{\boldsymbol{\mu}} - \tilde{\boldsymbol{\mu}}_h\|_{0,\Gamma} \\ &\leq \|\tilde{\boldsymbol{\mu}} - \boldsymbol{\omega}_h\|_1 + \tfrac{Ch^{1/2}}{\sqrt{\epsilon}}\|\tilde{\boldsymbol{\mu}} - \boldsymbol{\omega}_h\|_1 + C\|\tilde{\pi} - \lambda_h\|_0 \qquad \forall\, \boldsymbol{\omega}_h \in \mathbf{V}_h,\ \forall\, \lambda_h \in M_h\,. \end{aligned}$$

We estimate $\|\tilde{\pi} - \tilde{\pi}_h\|_0$ as follows. For an arbitrary $\lambda_h \in M_h$, using the equations for $\tilde{\boldsymbol{\mu}}$ and $\tilde{\boldsymbol{\mu}}_h$ and the inf-sup condition we deduce that

$$\begin{aligned} \|\tilde{\pi}_h - \lambda_h\|_0 &\leq C \sup_{\boldsymbol{\omega}_h \in \mathbf{V}_h} \frac{1}{\|\boldsymbol{\omega}_h\|_1}\Big((\nabla\tilde{\boldsymbol{\mu}} - \nabla\tilde{\boldsymbol{\mu}}_h, \nabla\boldsymbol{\omega}_h) + \frac{1}{\epsilon}(\tilde{\boldsymbol{\mu}} - \tilde{\boldsymbol{\mu}}_h, \boldsymbol{\omega}_h)_{0,\Gamma} + b(\boldsymbol{\omega}_h, \tilde{\pi} - \lambda_h)\Big) \\ &\leq C\Big(\|\nabla\tilde{\boldsymbol{\mu}} - \nabla\tilde{\boldsymbol{\mu}}_h\|_0 + \tfrac{1}{\epsilon}\|\tilde{\boldsymbol{\mu}} - \tilde{\boldsymbol{\mu}}_h\|_{-1/2,\Gamma} + \|\tilde{\pi} - \lambda_h\|_0\Big)\,. \end{aligned}$$

Using the triangle inequality and the fact that $\|\tilde{\boldsymbol{\mu}} - \tilde{\boldsymbol{\mu}}_h\|_{-1/2,\Gamma} \leq Ch\|\tilde{\boldsymbol{\mu}} - \tilde{\boldsymbol{\mu}}_h\|_1$ (see [8]), we conclude

$$\|\tilde{\pi} - \tilde{\pi}_h\|_0 \leq C\left(1 + \frac{h}{\epsilon}\right)\|\tilde{\boldsymbol{\mu}} - \tilde{\boldsymbol{\mu}}_h\|_1 + C\|\tilde{\pi} - \lambda_h\|_0 \qquad \forall\, \lambda_h \in M_h.$$

Combining the estimates for $(\tilde{\boldsymbol{\mu}} - \tilde{\boldsymbol{\mu}}_h)$ and $(\tilde{\pi} - \tilde{\pi}_h)$ and using the approximation properties for the spaces $\mathbf{V}_h$ and M_h, we obtain

$$\|\tilde{\boldsymbol{\mu}} - \tilde{\boldsymbol{\mu}}_h\|_1 + \|\tilde{\pi} - \tilde{\pi}_h\|_0 \leq C\left(1 + \frac{h^{1/2}}{\sqrt{\epsilon}} + \frac{h}{\epsilon}\right)h^m(\|\tilde{\boldsymbol{\mu}}\|_{m+1} + \|\tilde{\pi}\|_m).$$

Next, we estimate $\|\tilde{\mathbf{g}} - \tilde{\mathbf{g}}_h\|_{0,\Gamma}$. From the last equation of $(\mathrm{S}^*)_\epsilon$ and the last equation of $(\mathrm{S}_h^*)_\epsilon$, we easily obtain

$$\begin{aligned} &\beta^2\|\tilde{\mathbf{g}} - \tilde{\mathbf{g}}_h\|_{0,\Gamma}^2 + \tfrac{1}{\epsilon}(\tilde{\boldsymbol{\mu}} - \tilde{\boldsymbol{\mu}}_h, \tilde{\mathbf{g}} - \tilde{\mathbf{g}}_h)_{0,\Gamma} \\ &= \beta^2(\tilde{\mathbf{g}} - \tilde{\mathbf{g}}_h, \tilde{\mathbf{g}} - \mathbf{k}_h)_{0,\Gamma} + \tfrac{1}{\epsilon}(\tilde{\boldsymbol{\mu}} - \tilde{\boldsymbol{\mu}}_h, \tilde{\mathbf{g}} - \mathbf{k}_h)_{0,\Gamma} \qquad \forall\, \mathbf{k}_h \in \mathbf{V}_h\big|_\Gamma\,. \end{aligned}$$

Hence,

$$\|\tilde{\mathbf{g}}-\tilde{\mathbf{g}}_h\|_{0,\Gamma}^2 \le \frac{1}{\beta^2\epsilon}\|\tilde{\boldsymbol{\mu}}-\tilde{\boldsymbol{\mu}}_h\|_{0,\Gamma}\|\tilde{\mathbf{g}}-\tilde{\mathbf{g}}_h\|_{0,\Gamma}+\|\tilde{\mathbf{g}}-\tilde{\mathbf{g}}_h\|_{0,\Gamma}\|\tilde{\mathbf{g}}-\mathbf{k}_h\|_{0,\Gamma}+\frac{1}{\beta^2\epsilon}\|\tilde{\mathbf{g}}-\mathbf{k}_h\|_{0,\Gamma}\|\tilde{\boldsymbol{\mu}}-\tilde{\boldsymbol{\mu}}_h\|_{0,\Gamma}$$

so that

$$\begin{aligned}\|\tilde{\mathbf{g}}-\tilde{\mathbf{g}}_h\|_{0,\Gamma} &\le \tfrac{C}{\beta^2\epsilon}\|\tilde{\boldsymbol{\mu}}-\tilde{\boldsymbol{\mu}}_h\|_{0,\Gamma}+C\|\tilde{\mathbf{g}}-\mathbf{k}_h\|_{0,\Gamma}\\ &\le \tfrac{Ch^{1/2}}{\beta^2\epsilon}h^m\|\tilde{\boldsymbol{\mu}}\|_{m+1/2,\Gamma}+Ch^{m+1/2}\|\tilde{\mathbf{g}}\|_{m+1/2,\Gamma}\\ &\le Ch^m\left(h^{1/2}+\frac{h^{1/2}}{\beta^2\epsilon}\right)\left(\|\tilde{\boldsymbol{\mu}}\|_{m+1}+\|\tilde{\mathbf{u}}\|_{m+1}\right).\end{aligned}$$

We gain an additional half-order of h when estimating in $\mathbf{H}^{-1/2}(\Gamma)$-norm:

$$\|\tilde{\mathbf{g}}-\tilde{\mathbf{g}}_h\|_{-1/2,\Gamma} \le Ch^m\left(h+\frac{h}{\beta^2\epsilon}\right)\left(\|\tilde{\boldsymbol{\mu}}\|_{m+1}+\|\tilde{\mathbf{u}}\|_{m+1}\right).$$

Finally, we estimate $\tilde{\mathbf{u}}-\tilde{\mathbf{u}}_h$ and $\tilde{p}-\tilde{p}_h$. Again, we will use the techniques of the abstract approximation result of [6] with necessary modifications. We first derive

$$\begin{aligned}&\|\nabla\tilde{\mathbf{u}}-\nabla\tilde{\mathbf{u}}_h\|_0+\tfrac{1}{\sqrt{\epsilon}}\|\tilde{\mathbf{u}}-\tilde{\mathbf{u}}_h\|_{0,\Gamma}\\ &\le \|\nabla\tilde{\mathbf{u}}-\nabla\mathbf{z}_h\|_0+\tfrac{C}{\sqrt{\epsilon}}\|\tilde{\mathbf{u}}-\mathbf{z}_h\|_{0,\Gamma}+C\|\tilde{p}-r_h\|_0+\tfrac{C}{\sqrt{\epsilon}}\|\tilde{\mathbf{g}}-\tilde{\mathbf{g}}_h\|_{0,\Gamma} \qquad \forall\ \mathbf{z}_h\in\mathbf{Z}_h,\ \forall\ r_h\in M_h.\end{aligned}$$

Using the inf-sup condition we deduce

$$\inf_{\mathbf{z}_h\in\mathbf{Z}_h}\|\tilde{\mathbf{u}}-\mathbf{z}_h\|_1 \le C\inf_{\mathbf{w}_h\in\mathbf{V}_h}\|\tilde{\mathbf{u}}-\mathbf{w}_h\|_1$$

so that combining with the previous estimate and the fact that $\|\tilde{\mathbf{u}}-\mathbf{w}_h\|_{0,\Gamma} \le Ch^{1/2}\|\tilde{\mathbf{u}}-\mathbf{w}_h\|_1$ (see [8]), we are led to

$$\|\nabla\tilde{\mathbf{u}}-\nabla\tilde{\mathbf{u}}_h\|_0+\frac{1}{\sqrt{\epsilon}}\|\tilde{\mathbf{u}}-\tilde{\mathbf{u}}_h\|_{0,\Gamma} \le \|\tilde{\mathbf{u}}-\mathbf{w}_h\|_1+\frac{Ch^{1/2}}{\sqrt{\epsilon}}\|\tilde{\mathbf{u}}-\mathbf{w}_h\|_1+C\|\tilde{p}-r_h\|_0+\frac{C}{\sqrt{\epsilon}}\|\tilde{\mathbf{g}}-\tilde{\mathbf{g}}_h\|_{0,\Gamma}.$$

We now estimate $\|\tilde{p}-\tilde{p}_h\|_0$. From the equations for $\tilde{\mathbf{u}}$ and $\tilde{\mathbf{u}}_h$ and the inf-sup condition we deduce that

$$\begin{aligned}\|\tilde{p}_h-r_h\|_0 &\le C\sup_{\mathbf{w}_h\in\mathbf{V}_h}\frac{1}{\|\mathbf{w}_h\|_1}\Big((\nabla\tilde{\mathbf{u}}-\nabla\tilde{\mathbf{u}}_h,\nabla\mathbf{w}_h)\\ &+\frac{1}{\epsilon}(\tilde{\mathbf{u}}-\tilde{\mathbf{u}}_h,\mathbf{w}_h)_{0,\Gamma}+b(\mathbf{w}_h,\tilde{p}-r_h)+\frac{1}{\epsilon}(\tilde{\mathbf{g}}-\tilde{\mathbf{g}}_h,\mathbf{w}_h)_{0,\Gamma}\Big)\\ &\le C\Big(\|\nabla\tilde{\mathbf{u}}-\nabla\tilde{\mathbf{u}}_h\|_0+\frac{1}{\epsilon}\|\tilde{\mathbf{u}}-\tilde{\mathbf{u}}_h\|_{-1/2,\Gamma}+\|\tilde{p}-r_h\|_0+\frac{1}{\epsilon}\|\tilde{\mathbf{g}}-\tilde{\mathbf{g}}_h\|_{-1/2,\Gamma}\Big).\end{aligned}$$

Using the triangle inequality and the fact that $\|\tilde{\mathbf{u}}-\tilde{\mathbf{u}}_h\|_{-1/2,\Gamma} \le Ch\|\tilde{\mathbf{u}}-\tilde{\mathbf{u}}_h\|_1$ (see [8]), we conclude

$$\|\tilde{p}_h-r_h\|_0 \le C\left(1+\frac{h}{\epsilon}\right)\|\tilde{\mathbf{u}}-\tilde{\mathbf{u}}_h\|_1+C\|\tilde{p}-r_h\|_0+C\frac{1}{\epsilon}\|\tilde{\mathbf{g}}-\tilde{\mathbf{g}}_h\|_{-1/2,\Gamma}+\frac{C}{\sqrt{\epsilon}}\|\tilde{\mathbf{g}}-\tilde{\mathbf{g}}_h\|_{0,\Gamma}.$$

Combining estimates for $(\tilde{\mathbf{u}}-\tilde{\mathbf{u}}_h)$, $(\tilde{p}-\tilde{p}_h)$, and $(\tilde{\mathbf{g}}-\tilde{\mathbf{g}}_h)$ and using the approximation properties for the spaces $\mathbf{V}_h$ and M_h, we obtain

$$\|\tilde{\mathbf{u}}-\tilde{\mathbf{u}}_h\|_1+\|\tilde{p}-\tilde{p}_h\|_0 \le Ch^m\left(1+\frac{h^{1/2}}{\sqrt{\epsilon}}+\frac{h}{\epsilon}+\frac{h}{\epsilon^2}+\frac{h^{1/2}}{\epsilon\sqrt{\epsilon}}\right) \times\Big(\|\tilde{\mathbf{u}}\|_{m+1}+\|\tilde{p}\|_m+\|\tilde{\boldsymbol{\mu}}\|_{m+1}+\|\tilde{\pi}\|_m\Big).$$

To summarize, we have shown that

$$\|\tilde{\mathbf{u}}-\tilde{\mathbf{u}}_h\|_1+\tfrac{1}{\sqrt{\epsilon}}\|\tilde{\mathbf{u}}-\tilde{\mathbf{u}}_h\|_{0,\Gamma}+\|\tilde{p}-\tilde{p}_h\|_0+\|\tilde{\boldsymbol{\mu}}-\tilde{\boldsymbol{\mu}}_h\|_1+\tfrac{1}{\sqrt{\epsilon}}\|\tilde{\boldsymbol{\mu}}-\tilde{\boldsymbol{\mu}}_h\|_{0,\Gamma}+\|\tilde{\pi}-\tilde{\pi}_h\|_0$$

$$\le Ch^m\left(1+\frac{h^{1/2}}{\sqrt{\epsilon}}+\frac{h}{\epsilon}+\frac{h}{\epsilon^2}+\frac{h^{1/2}}{\epsilon\sqrt{\epsilon}}\right)\Big(\|\tilde{\mathbf{u}}\|_{m+1}+\|\tilde{p}\|_m+\|\tilde{\boldsymbol{\mu}}\|_{m+1}+\|\tilde{\pi}\|_m\Big).$$

Setting $\epsilon=\mathcal{O}(h^{1/3})$ we obtain (4.1). ∎

We now turn to the derivation of the error estimate for the approximation of $(\mathrm{S}^*)_\epsilon$.

THEOREM 4.2. *Let $(\mathbf{u},p,\boldsymbol{\mu},\pi)\in\mathbf{H}^{m+1}(\Omega)\times H^m(\Omega)\times\mathbf{H}^{m+1}(\Omega)\times H^m(\Omega)\times$ be a solution of $(S^*)_\epsilon$. Then under suitable assumptions on $\mathcal{F}(\cdot)$, there exists a solution $(\mathbf{u}_h,p_h,\boldsymbol{\mu}_h,\pi_h)\in\mathbf{V}_h\times M_h\times\mathbf{V}_h\times M_h$ to the system $(S_h^*)_\epsilon$ satisfying the following estimate:*

$$\|\tilde{\mathbf{u}}-\tilde{\mathbf{u}}_h\|_1+\|\tilde{p}-\tilde{p}_h\|_0+\|\tilde{\boldsymbol{\mu}}-\tilde{\boldsymbol{\mu}}_h\|_1+\|\tilde{\pi}-\tilde{\pi}_h\|_0\le Ch^m(\|\tilde{\mathbf{u}}\|_{m+1}+\|\tilde{p}\|_m+\|\tilde{\boldsymbol{\mu}}\|_{m+1}+\|\tilde{\pi}\|_m).$$

Proof. Defining the operator G by

$$\begin{aligned}\langle G(\mathbf{u},\boldsymbol{\mu}),(\mathbf{v},\mathbf{w})\rangle &= c_1(\mathbf{u}^c,\mathbf{u},\mathbf{v})+c_1(\mathbf{u},\mathbf{u}^c,\mathbf{v})-c_1(\mathbf{u}^c,\mathbf{u}^c,\mathbf{v})-(\mathbf{f},\mathbf{v})\\ &\quad+c_1(\mathbf{u}^c,\mathbf{w},\boldsymbol{\mu}-\boldsymbol{\mu}^c)+c_1(\mathbf{w},\mathbf{u}^c,\boldsymbol{\mu}-\boldsymbol{\mu}^c)\\ &\quad+c_1(\mathbf{u},\mathbf{w},\boldsymbol{\mu}^c)+c_1(\mathbf{w},\mathbf{u},\boldsymbol{\mu}^c)-\langle\mathcal{F}_{\mathbf{u}}(\mathbf{u}^c),\mathbf{w}\rangle-\langle\mathcal{F}_{\mathbf{uu}}(\mathbf{u}^c)(\mathbf{u}-\mathbf{u}^c),\mathbf{w}\rangle,\end{aligned}$$

we see that $(\mathrm{S}^*)_\epsilon$ and $(\mathrm{S}_h^*)_\epsilon$ can be rewritten as $(\mathbf{u},p,\boldsymbol{\mu},\pi)+TG(\mathbf{u},p,\boldsymbol{\mu},\pi)=0$ and $(\mathbf{u}_h,p_h,\boldsymbol{\mu}_h,\pi_h)+T_hG(\mathbf{u}_h,p_h,\boldsymbol{\mu}_h,\pi_h)=0$, respectively. The assumptions of Brezzi–Rappaz–Raviart theory (see [6]) are readily verified under appropriate assumptions on $\mathcal{F}$. Hence, applying that theory we immediately obtain the error estimate for the approximation of $(\mathrm{S}^*)_\epsilon$:

$$\begin{aligned}&\|\mathbf{u}-\mathbf{u}_h\|_1+\|p-p_h\|_0+\|\boldsymbol{\mu}-\boldsymbol{\mu}_h\|_1+\|\pi-\pi_h\|_0\\ &\le Ch^m(\|\mathbf{u}\|_{m+1}+\|p\|_m+\|\boldsymbol{\mu}\|_{m+1}+\|\pi\|_m).\end{aligned}$$ ∎

Remark. Using similar techniques and by some additional manipulations we can derive similar error estimates for the approximation of (S) and $(\mathrm{S})_\epsilon$.

We now comment on some implementational issues of the finite element versions of the SQP methods. We use continuous piecewise quadratics for the velocity $\mathbf{u}$ and for the adjoint velocity $\boldsymbol{\mu}$, and continuous piecewise linear functions for the pressure p and adjoint pressure π; the same triangular grid is used for both finite element spaces; see Figure 22. This choice of spaces complies with the *div-stability condition*. For the approximation of integrals we used a seven point quadrature rule for triangular regions. For the solution of the discretized system of algebraic equations, we use banded Gaussian elimination with partial pivoting.

The SQP algorithms presented in the previous section are not sufficient for convergence to a minimum point from arbitrary initial guesses. As mentioned previously, outside the contraction ball one has to rely on line search to compute the step length η and inside the ball one sets $\eta = 1$.

In our computations, we use a continuation method on the Reynolds number as a globalization strategy which we briefly describe here. Set $\eta = 1$ in the SQP algorithms. Let R_f be the desired Reynolds number at which we want to solve the optimal control problem. We start with $Re = 0$ and define a sequence of optimal control problems by increasing the Reynolds number with increment ΔRe. When $Re = 0$ the optimal control problems (P), $(\mathrm{P})_\epsilon$, and $(\mathrm{P}^*)_\epsilon$ are linear quadratic programming problems which can be solved in one step. For subsequent optimization problems we choose sufficiently small ΔRe (the increment of the Reynolds number) such that the solution obtained by solving the ith sequence in the optimization problem with Reynolds number defined by $i\Delta Re$ can be used as the initial iterate for the $(i+1)$th problem to achieve convergence—at least when we are away from the limit and bifurcation points.

5. Numerical results. In this section we report and discuss computational results for three test problems. Each of the test problems serves a different purpose. Test Problem I demonstrates potential applications of optimal control techniques to engineering problems. The geometry is a typical test domain used by CFD researchers, and the uncontrolled simulations on such a domain were well documented in the literature. Our simulations for the controlled flows are compared with the simulation results for the uncontrolled flows. Problem I could be solved by using any of the three algorithms proposed in section 3, but we used only Algorithm A3. With Test Problem II we intend to confirm numerically the convergence (as $\epsilon \to 0$) of solutions of the penalized optimal control problems. Such convergence results were shown in [13] under certain restrictions on the functionals and the data. In Test Problem III, we intend to establish the convergence results for general functionals and general data that do not necessarily satisfy the theoretical assumptions of [13]. Thereby we establish the applicability of our algorithms to general boundary flow control problems. Also, the performances of the three algorithms for Test Problem III are compared and evaluated.

5.1. Test problem I. In this test example, we consider vorticity minimization in fluid flows. We choose the two-dimensional flow in a backward-facing step channel as our flow setting. A schematic of the geometry is given in Figure 1. The height of the inflow boundary is 0.5 and that of the outflow boundary is 1. The length of the narrower section of the channel is 1 and that of the wider section of the channel is 7 (the total horizontal length is 8). At the inflow we assume the flow is parabolic and we take $\mathbf{u}(y) = \mathbf{u}_i = 8(y-0.5)(1-y)$ (the coordinate system is chosen such that $y = 1$ on the top boundary). At the outflow boundary, we again assume the flow is parabolic and $\mathbf{u} = \mathbf{u}_o = y(1-y)$. We define the Reynolds number as $Re = \frac{V_{max} \cdot H}{\nu}$, where V_{max} = maximum inlet velocity, H = channel height, and ν = kinematic viscosity of the fluid. We choose throughout this simulation $V_{max} = \frac{1}{2}$ and $H = 1$ with a corresponding $Re = \frac{1}{2\nu}$. It is well known that beyond a certain Reynolds number the flow separates and a recirculation forms near the corner region. A number of studies have been devoted to this problem and various investigations have been done; see, for example, [7] and [4]. We choose the Reynolds number to be in the range of 200–400. For this range the flow is known to be steady and two-dimensional; see [7] and [4]. Simulations of uncontrolled flows for $Re = 200$, $Re = 300$, and $Re = 400$ are depicted

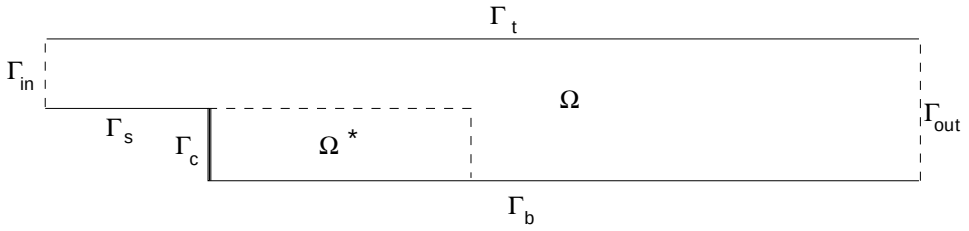

FIG. 1. *Computational domain* Ω *for channel flow.*

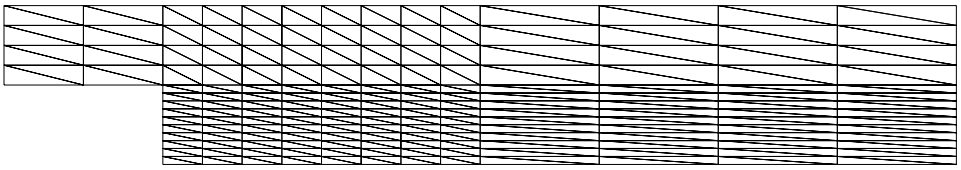

FIG. 2. *Finite element grid for the channel geometry.*

in Figures 3, 10, and 12, respectively.

We will demonstrate that, by introducing the boundary velocity control, the vorticity development near the corner can be damped out. To achieve this goal, we formulate an optimal control problem that involves the vorticity in the region where we want to damp out the vorticity. Specifically, the control problem is posed as follows: Minimize the functional

$$\mathcal{J}(\mathbf{u}, \mathbf{g}) = \frac{1}{2} \int_{\Omega^*} |\nabla \times \mathbf{u}|^2 \, d\Omega + \frac{\beta^2}{2} \int_{\Gamma_c} |\mathbf{g}|^2 \, d\Gamma$$

subject to the constraints (2.11)–(2.12) defined in the channel. Here Ω^* is the corner region of the channel and is chosen to be $\Omega^* = (1, 3) \times (0, 0.5)$; see Figure 1. The portion of boundary Γ_c where control is applied is taken to be the line segment between $y = 0$ and $y = 0.5$ at $x = 1$ as shown in Figure 1. Note that for this cost functional,

$$\langle \mathcal{F}_{\mathbf{u}}(\mathbf{u}, p), \mathbf{w} \rangle = \int_{\Omega^*} (\nabla \times \mathbf{u}) \cdot (\nabla \times \mathbf{w}) \, d\Omega$$

and

$$\langle \mathcal{F}_p(\mathbf{u}, p), r \rangle = 0 \,.$$

Three different case studies were conducted.

- Case A (U control): *suction/blowing of mass* at the control portion with tangential velocity $V = 0$ (i.e., normal velocity control).
- Case B (U,V control): *suction/blowing of mass* at the control portion with velocity $U \neq 0$ and $V \neq 0$ (i.e., full boundary velocity control).
- Case C (V control): *tangential movement of boundary surfaces* at the control portion with normal velocity $U = 0$ (i.e., tangential velocity control).

The computational domain is divided into 332 triangles with finer mesh around the corner of the step; see Figure 2. For each of these test cases, we applied Algorithm A3 to find the optimal controls and optimal flow fields. The parameter in the functional was chosen as $\beta^2 = 0.1$. The penalty parameter was taken to be $\epsilon = 0.00001$.

TABLE 1
The $\mathbf{L}^2(\Omega)$-norm of the vorticity for the three test cases.

Case	A (U control)	B (U, V control)	C (V) control
Uncontrolled vorticity	0.5930	0.5930	0.5930
Controlled vorticity	0.3979	0.3931	0.434

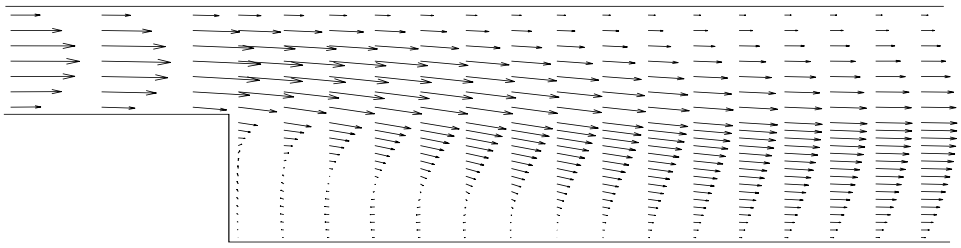

FIG. 3. *The velocity field for the uncontrolled case at $Re = 200$.*

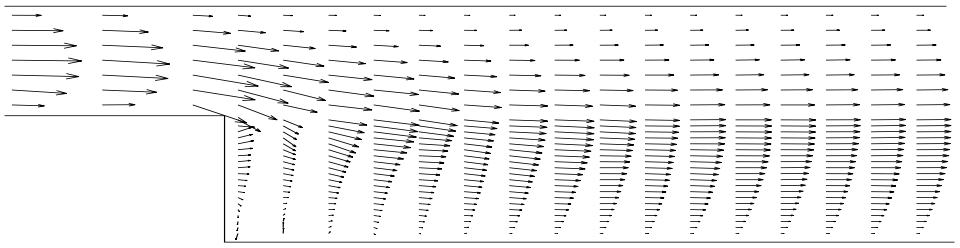

FIG. 4. *The velocity field for the controlled case at $Re = 200$: U control.*

Convergence was obtained in seven SQP iterations in all three cases (Cases A, B, C), and the CPU time was 40.29 minutes on IBM RISC 6000/390. The values of the vorticity $\int_{\Omega^*} |\nabla \times \mathbf{u}|^2 \, d\Omega$ with and without controls are tabulated in Table 1 for all three cases. The computed values of the vorticity of optimal solutions for Cases A, B, and C indicate that the minimization effects of the vorticity in all three cases are comparable. The optimal flow fields in all three cases are depicted in Figures 4, 5, and 6, respectively. For comparison, the uncontrolled velocity field is shown in Figure 3. The controls that should be applied in each case (in order to obtain the optimal flow field) are shown in Figures 7, 8, and 9, respectively. The choice of the type of velocity control (normal, tangential, or full velocity control) should be decided based on which type is the easiest to apply in the particular application.

We also performed simulations with different Reynolds numbers to verify the performance of the algorithm. The resulting flow fields along with the uncontrolled fields are given in Figures 10–13 for various Reynolds numbers, and the corresponding vorticity values are given in Table 2. For these simulations we used U control only.

The numerical experiments demonstrate that the vorticity level (or the flow recirculation) in the domain can be successfully damped out by applying boundary controls on part of the boundary.

5.2. Test problem II. In this section, we intend to validate numerically the convergence results established in [13] so as to ensure that Algorithm A2 or A3 can be used reliably by fixing a sufficiently small ϵ.

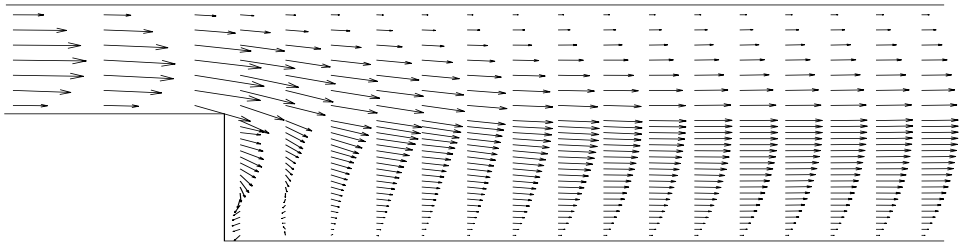

FIG. 5. *The velocity field for the controlled case at* $Re = 200$*: (U,V) control.*

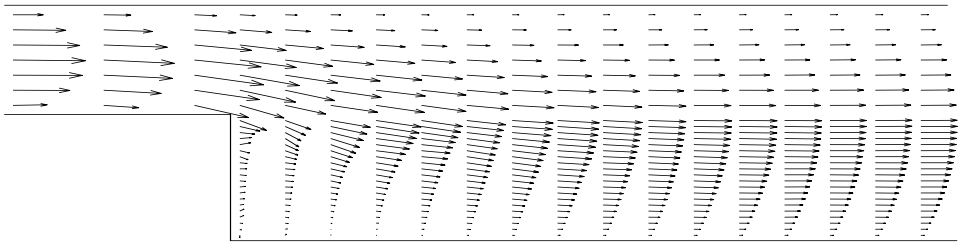

FIG. 6. *The velocity field for the controlled case at* $Re = 200$*: V control.*

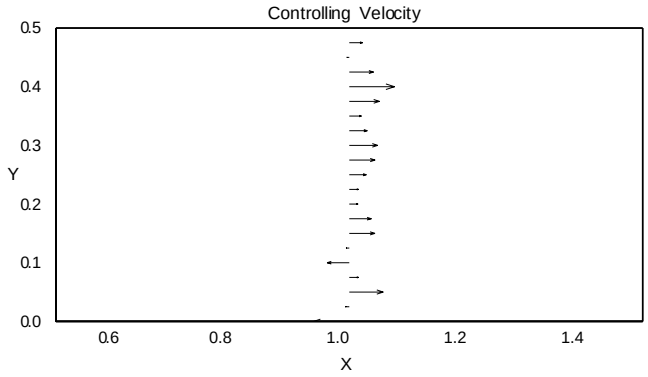

FIG. 7. *The controlling velocity: U control.*

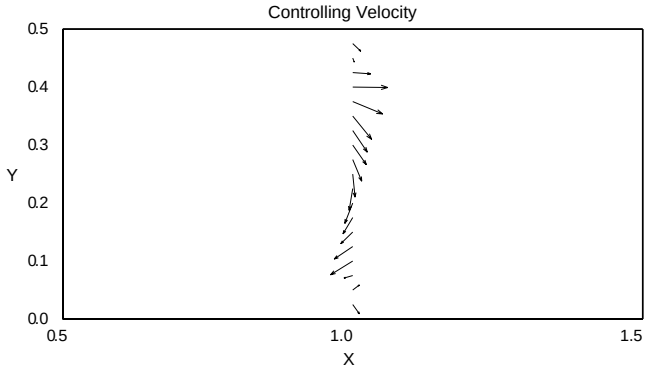

FIG. 8. *The controlling velocity: (U,V) control.*

TABLE 2
The $\mathbf{L}^2(\Omega)$-norm of the vorticity for different Reynolds numbers.

Reynolds number	200	300	400
Uncontrolled vorticity	0.59	0.72	0.84
Controlled vorticity	0.39	0.45	0.53

We consider the minimization of vorticity in a simple geometry, that is, a unit square: minimize

$$\mathcal{J}(\mathbf{u}, \mathbf{g}) = \frac{1}{2} \int_\Omega |\nabla \times \mathbf{u}|^2 \, d\Omega + \frac{\beta^2}{2} \int_\Gamma |\mathbf{g}|^2 \, d\Gamma$$

subject to the constraints (2.11)–(2.12) defined on the unit square. Again we note that

$$\langle \mathcal{F}_\mathbf{u}(\mathbf{u}, p), \mathbf{w} \rangle = \int_\Omega (\nabla \times \mathbf{u}) \cdot (\nabla \times \mathbf{w}) \, d\Omega$$

and

$$\langle \mathcal{F}_p(\mathbf{u}, p), r \rangle = 0 \, .$$

The computations were done with both Algorithms A2 and A3. The following data were used in the simulations: Ω is the unit square; $\nu = 0.1$; and the prescribed body force $\mathbf{f} = (f_1, f_2)^T$, where

$$\mathbf{f} = \begin{pmatrix} -50\nu\pi \cos((x-0.25)\pi/0.4) \sin((y-0.25)\pi/0.4) - \frac{20}{\pi} \sin((x-0.25)\pi/0.2) \\ 50\nu\pi \sin((x-0.25)\pi/0.4) \cos((y-0.25)\pi/0.4) - \frac{20}{\pi} \sin((y-0.25)\pi/0.2) \end{pmatrix}$$

in the region $\{(x, y) : |x - 0.25| \le 0.2, |y - 0.25| \le 0.2\}$; and $\mathbf{f} = (-0.25x, -0.25y)^T$ elsewhere on the unit square. In the cost functional we chose $\beta^2 = 0.01$. We used a uniform mesh in Ω with 162 triangles. We computed the optimal solutions for a sequence of ϵ values by implementing Algorithms A2 and A3: $\epsilon_1 = 1$, $\epsilon_2 = 10^{-1}$, $\epsilon_3 = 10^{-2}$, $\epsilon_4 = 10^{-3}$, $\epsilon_5 = 10^{-4}$, $\epsilon_6 = 10^{-5}$, $\epsilon_7 = 10^{-6}$, and $\epsilon_8 = 10^{-7}$. We also computed the $\mathbf{L}^2(\Omega)$-norms of $\nabla \times \widehat{\mathbf{u}}_{\epsilon_i}$ as shown in Table 3. The $\mathbf{L}^2(\Omega)$-norm of the vorticity of the uncontrolled velocity field is 39.77.

Figure 14 shows the uncontrolled flow field. Figures 15–19 depict the optimal velocity fields for various ϵ values we tested. We could easily visualize from these figures the convergence of the optimal solutions as $\epsilon \to 0$. Also, by comparing the uncontrolled flow field with the optimal flow fields (for small ϵ), we clearly see the damping of vorticity level in the optimal control solutions. We obtained convergence in six SQP iterations on IBM RISC 6000/390 and the CPU time was 4.25 minutes.

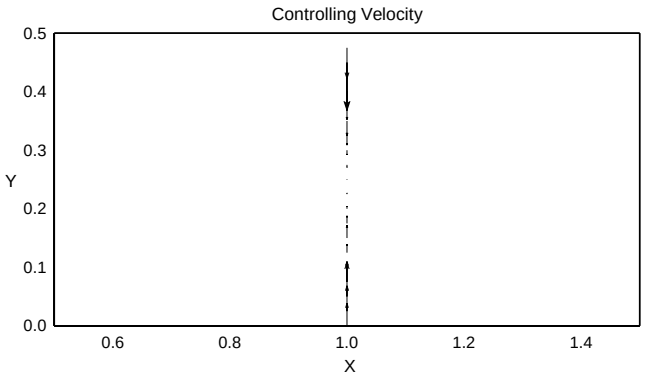

FIG. 9. *The controlling velocity: V control.*

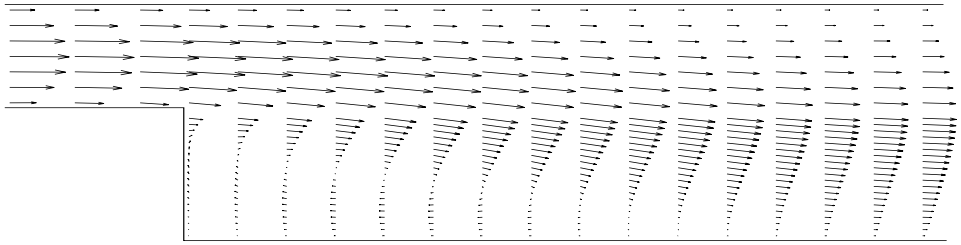

FIG. 10. *The velocity field for the uncontrolled case at* $Re = 300$.

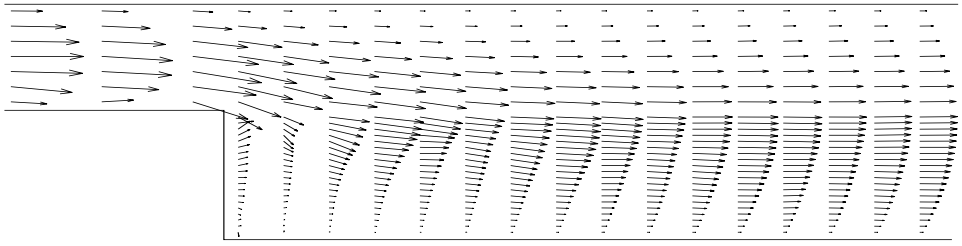

FIG. 11. *The velocity field for the controlled case at* $Re = 300$*: U control.*

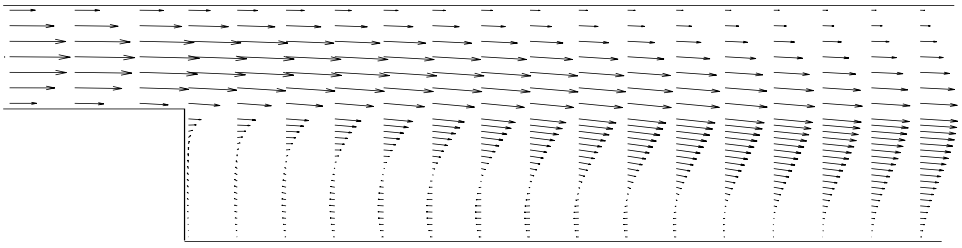

FIG. 12. *The velocity field for the uncontrolled case at* $Re = 400$.

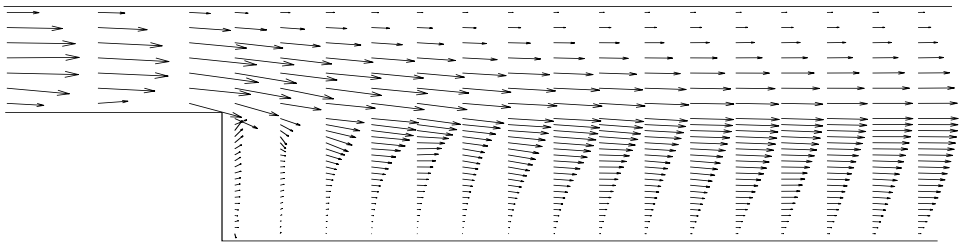

FIG. 13. *The velocity field for the controlled case at* $Re = 400$*: U control.*

TABLE 3
The $\mathbf{L}^2(\Omega)$*-norm of the vorticity of optimal solutions.*

ϵ_i	1	10^{-1}	10^{-2}	10^{-3}	10^{-4}	10^{-5}	10^{-6}	10^{-7}
$\left\|\nabla\times\mathbf{u}_\epsilon\right\|^2_{\mathbf{L}^2}$	12.20	11.81	11.64	11.63	11.62	11.62	11.62	11.62

5.3. Test problem III. In this test problem, we will compare the three different approaches described in section 2 (or the three different algorithms described in section 3) on the following optimal control problem of tracking type. The control objective can be stated as follows: Given a desired velocity profile, find the boundary velocity such that the velocity in the flow domain is as close as possible to the desired one. We formulate the control problem in the form of (P), $(P)_\epsilon$, or $(P^*)_\epsilon$ with $\mathcal{F}(\mathbf{u}, p) = \frac{1}{2}\int_\Omega |\mathbf{u} - \mathbf{u}_d|^2\, d\Omega$.

The computational domain is taken to be a unit square and the desired flow field is chosen as

$$\mathbf{u}_d(\mathbf{x}) = \begin{pmatrix} \varphi_y(x,y) \\ -\varphi_x(x,y) \end{pmatrix},$$

where φ is the stream function which is taken to be $\varphi(x,y) = \frac{1}{2\pi}\sin(2\pi y)(\cos(2\pi x) - 1)$. We choose the viscosity $\nu = \frac{1}{Re} = 0.01$ and the parameter $\beta^2 = .01$. Figure 20 gives the desired velocity field $\mathbf{u}_d$. The computed optimal flow field with Approach I is shown in Figure 21; the computed parameter γ in (3.6) is $\gamma = 0.655$. The controlled velocity field is in nice agreement with the target field. Table 4 presents the CPU time in minutes and number of iterations for each of the approaches. According to this table Approaches II and III were clearly superior to Approach I. Thus these two approaches are not only convenient to implement but also reduce the computational time.

Remark. As indicated in the Introduction, the parameter β^2 in the functional changes the weight of the two terms in the functional and affects the size of control to be applied. In each example, we compared the performance of several different values of β and chose one that minimized the vorticity quantity. For instance, in Test Problem I, $\beta^2 = 0.1$ was chosen; and in Test Problems II and III, $\beta^2 = 0.01$ was chosen.

TABLE 4
The $\mathbf{L}^2(\Omega)$-norm of the vorticity of optimal solutions for the three test problems.

Approach	I (P)	II $(P)_\epsilon$	III $(P^*)_\epsilon$
CPU	6.15	2.06	1.01
No. of iterations	5	10	5

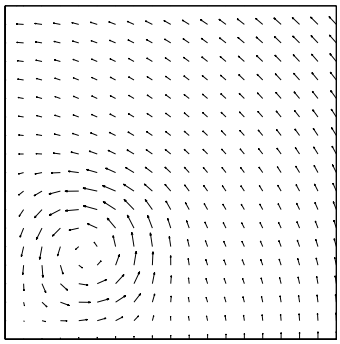

FIG. 14. *Uncontrolled velocity field.*

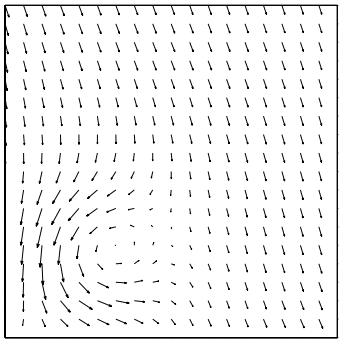

FIG. 15. *Optimal velocity field* ($\epsilon = 1$).

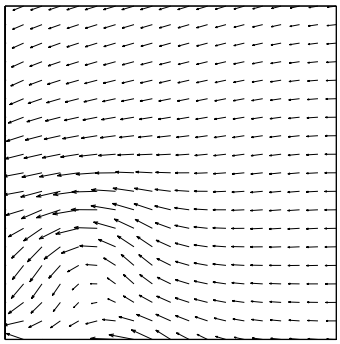

FIG. 16. *Optimal velocity field* ($\epsilon = 10^{-1}$).

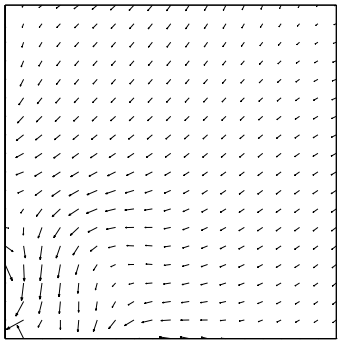

FIG. 17. *Optimal velocity field* ($\epsilon = 10^{-3}$).

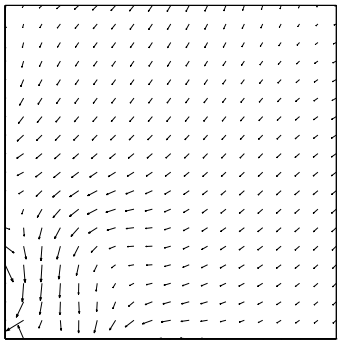

FIG. 18. *Optimal velocity field* ($\epsilon = 10^{-5}$).

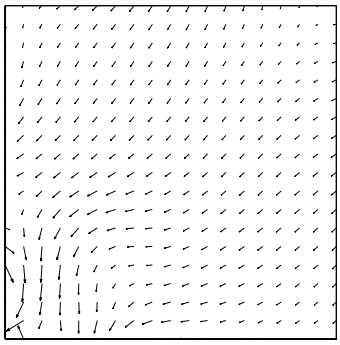

FIG. 19. *Optimal velocity field* ($\epsilon = 10^{-7}$).

6. Conclusion. We presented a penalized Neumann control approach for solving Dirichlet control problems and demonstrated its feasibility, via computational experiments, on certain boundary control problems for fluid flows governed by the Navier–Stokes equations. The numerical results unequivocally confirm not only the theoretical convergence results but also the applicability of the penalized approach for solving optimal flow control problems. The computational experiments reported

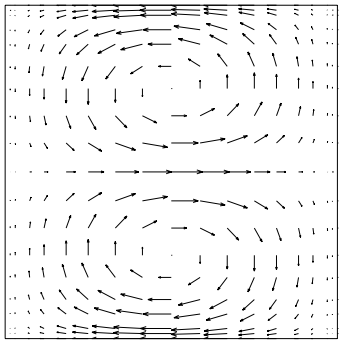

FIG. 20. *The desired velocity field.*

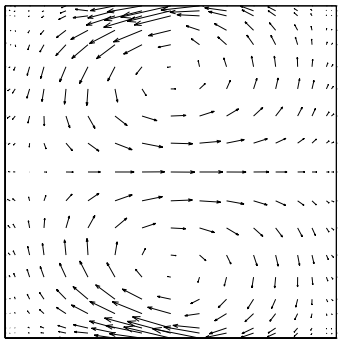

FIG. 21. *The velocity field for the controlled flow.*

in this paper also demonstrate the effectiveness of the optimal flow control techniques and suggest the potential application of optimal flow control methodology for realistic engineering problems. The following points about the penalty methods are of particular importance:

- The penalty method gives a numerically convenient and effective treatment of the Dirichlet boundary control problems.
- The optimal solutions obtained by the penalty method generally converge to a true optimal solution of the original unpenalized problem as the penalty constant $\epsilon \to 0$.
- In practical implementation, one needs only to choose a sufficiently small ϵ and solve for the corresponding optimal solution. When finite element discretization is used to solve the partial differential systems of equations involved, a rule of thumb for choosing the ϵ is for ϵ to be of order $h^{1/3}$, where h is a measure of the grid size.
- SQP algorithms provide an efficient solution method for the penalized optimal control problems.
- The linear penalty method, i.e., (2.10), generally works as well as the nonlinear penalty method, i.e., (2.6).
- The choice of the parameter β affects the optimal solution obtained. For different problems, we need to choose the parameter β suitably.

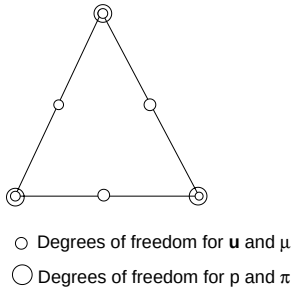

FIG. 22. *Degrees of freedom for* $\mathbf{u}$, p, π, *and* $\boldsymbol{\mu}$.

REFERENCES

[1] I. BABUŠKA, *The finite element method with penalty*, Math. Comp., 27 (1973), pp. 221–228.
[2] R. FLETCHER, *Practical Methods of Optimization*, *Vol.* 2. *Constrained Optimization*, John Wiley & Sons, New York, 1981.
[3] H. O. FATTORINI AND S. S. SRITHARAN, *Existence of optimal controls for viscous flow problems*, Proc. Roy. Soc. London Ser. A, 439 (1992), pp. 81–102.
[4] D. K. GARTLING, *A test problem for outflow boundary conditions-flow over a backward facing step*, Internat. J. Numer. Methods Fluids, 11 (1990), pp. 953–967.
[5] P. E. GILL, W. MURRAY, AND M. H. WRIGHT, *Practical Optimization*, Academic Press, New York, 1989.
[6] V. GIRAULT AND P.-A. RAVIART, *Finite Element Methods for Navier-Stokes Equations*, Springer-Verlag, Berlin, 1986.
[7] P. M. GRESHO, D. K. GARTLING, J. R. TORCZYNSKI ET AL., *Is the steady viscous incompressible two-dimensional flow over a backward-facing step at Re=800 stable*, Inter. J. Numer. Methods Fluids, 17 (1993), pp. 501–541.
[8] M. D. GUNZBURGER AND L. S. HOU, *Treating inhomogeneous essential boundary conditions in finite element and calculation of boundary stresses*, SIAM J. Numer. Anal., 29 (1992), pp. 390–424.
[9] M. D. GUNZBURGER, *Finite Element Methods for Viscous Incompressible Flows*, Academic Press, London, 1989.
[10] M. D. GUNZBURGER, ED., *Flow Control*, IMA Vol. Math. Appl. 68, Springer-Verlag, New York, 1995.
[11] M. D. GUNZBURGER, L. S. HOU, AND T. SVOBODNEY, *Analysis and finite element approximation of optimal control problems for the stationary Navier-Stokes equations with Dirichlet controls*, Modél. Math. Anal. Numér., 25 (1991), pp. 711–748.
[12] M. D. GUNZBURGER, L. S. HOU, AND T. SVOBODNEY, *Analysis and finite element approximation of optimal control problems for the stationary Navier-Stokes equations with distributed and Neumann controls*, Math. Comp., 57 (1991), pp. 123–151.
[13] L. S. HOU AND S. S. RAVINDRAN, *A penalized Neumann control approach for solving an optimal Dirichlet control problem for the Navier–Stokes equations*, SIAM J. Control Optim., 36 (1998), pp. 1795–1814.
[14] L. S. HOU AND S. S. RAVINDRAN, *Computations of boundary optimal control problems for an electrically conducting fluid*, J. Comput. Phys., 128 (1996), pp. 319–330.
[15] K. ITO AND S. S. RAVINDRAN, *Optimal control of thermally convected fluid flows*, SIAM J. Sci. Comput., 19 (1998), pp. 1847–1869.
[16] S. S. RAVINDRAN, *Numerical solution of optimal control for thermally convected fluid flow*, Internat. J. Numer. Methods Fluids, 25 (1997), pp. 205–223.
[17] Y. R. OU, *Mathematical modeling and numerical simulation in external flow control*, in Flow Control, IMA Vol. Math. Appl. 68, M.D. Gunzburger, ed., Springer-Verlag, New York, 1995, pp. 219–253.
[18] S. S. SRITHARAN, *Dynamic programming of the Navier-Stokes equations*, System Control Lett., 16 (1991), pp. 299–307.
[19] S. S. SRITHARAN, ED., *Optimal Control of Viscous Flows*, SIAM, Philadelphia, PA, 1998.
[20] S. S. SRITHARAN, *Optimal feedback control of hydrodynamics: A progress report*, in Flow Control, IMA Vol. Math. Appl. 68, M. D. Gunzburger, ed., Springer-Verlag, New York, 1995, pp. 257–274.